176600-12-F

Final Report

SENSOR SUPPORT FOR THE DARPA AUTONOMOUS LAND VEHICLE PROGRAM

STAFF REPORT

Sensor Systems Division

OCTOBER 1988

Prepared for:
Defense Advanced Research Projects Agency
1400 Wilson Boulevard
Arlington, VA 22209
DARPA Order 4670

Issued by:
U.S. Army Tank Automotive Command
Warren, MI 48090

Contract DAAE07-86-C-R019

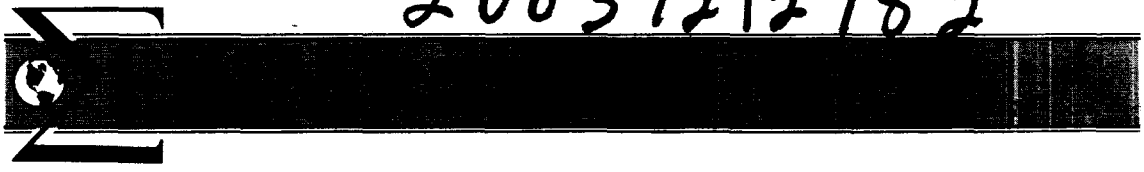

REPORT DOCUMENTATION PAGE

1a. REPORT SECURITY CLASSIFICATION Unclassified	1b. RESTRICTIVE MARKINGS
2a. SECURITY CLASSIFICATION AUTHORITY	3. DISTRIBUTION/AVAILABILITY OF REPORT Approved for Public Release Distribution Unlimited
2b. DECLASSIFICATION/DOWNGRADING SCHEDULE	
4. PERFORMING ORGANIZATION REPORT NUMBER(S) 176600-12-F	5. MONITORING ORGANIZATION REPORT NUMBER(S)
6a. NAME OF PERFORMING ORGANIZATION Environmental Research Institute of Michigan 6b. OFFICE SYMBOL (if applicable)	7a. NAME OF MONITORING ORGANIZATION USA TACOM, AMSTA-ZSS (Tibor F. Czako)
6c. ADDRESS (City, State, and ZIP Code) P. O. Box 8618 Ann Arbor, MI 48107	7b. ADDRESS (City, State, and ZIP Code) Warren, MI 48090
8a. NAME OF FUNDING/SPONSORING ORGANIZATION DARPA 8b. OFFICE SYMBOL (if applicable)	9. PROCUREMENT INSTRUMENT IDENTIFICATION NUMBER DARPA Order 4670
8c. ADDRESS (City, State, and ZIP Code) 1400 Wilson Blvd. Arlington, VA 22209	10. SOURCE OF FUNDING NUMBERS PROGRAM ELEMENT NO / PROJECT NO. / TASK NO. / WORK UNIT ACCESSION NO.
11. TITLE (Include Security Classification) Sensor Support for the DARPA Autonomous Land Vehicle Program	
12. PERSONAL AUTHOR(S) K. Gleichman, L. Harmon, T. Miciek, C. Miller, D. Zuk	
13a. TYPE OF REPORT Final 13b. TIME COVERED FROM 7/84 TO 8/87 14. DATE OF REPORT (Year, Month, Day) October 1988 15. PAGE COUNT 69	
16. SUPPLEMENTARY NOTATION	

17. COSATI CODES		
FIELD	GROUP	SUB-GROUP
17	5	
15	3	

18. SUBJECT TERMS (*Continue on reverse if necessary and identify by block number*)
Laser radar, vision sensors, 3-D sensor, active sensor, multispectral sensor, autonomous land vehicle, ALV

19. ABSTRACT (*Continue on reverse if necessary and identify by block number*)

Final report on vision-sensor support for the DARPA Autonomous Land Vehicle (ALV) program. ERIM fabricated three laser-ranging sensors (0.82 micron) for the program and one active multispectral ranging (MS) sensor. This report describes the sensors and support provided to the ALV contractors receiving the sensors during the period July 1984 through August 1987. The MS sensor was given only limited laboratory testing and never adapted to the autonomous vehicle. The report also discusses on-going research related to diode-pumped lasers.

20. DISTRIBUTION/AVAILABILITY OF ABSTRACT ☐ UNCLASSIFIED/UNLIMITED ☒ SAME AS RPT ☐ DTIC USERS	21. ABSTRACT SECURITY CLASSIFICATION Unclassified
22a. NAME OF RESPONSIBLE INDIVIDUAL Tibor F. Czako	22b. TELEPHONE (Include Area Code) (313) 574-5515 22c. OFFICE SYMBOL AMSTA-ZSS

(THIS PAGE INTENTIONALLY LEFT BLANK)

TABLE OF CONTENTS

(THIS PAGE INTENTIONALLY LEFT BLANK)

LIST OF ILLUSTRATIONS

(THIS PAGE INTENTIONALLY LEFT BLANK)

LIST OF TABLES

(THIS PAGE INTENTIONALLY LEFT BLANK)

SECTION I
INTRODUCTION

The Defense Advanced Research Projects Agency's (DARPA) Strategic Computing Program [1] has, as one of its feasibility demonstrations, the development of an Autonomous Land Vehicle (ALV) system including associated vision sensors.

ERIM has pioneered in the field of 3D sensor technology since the mid-1970's [2,3,4]. In 1982, DARPA contracted with ERIM to investigate the possible use of a 3D sensor as the "vision" system for the Adaptive Suspension Vehicle (ASV) being constructed for DARPA by Ohio State University (OSU)[5].

---

1. "Strategic Computing", Defense Advanced Research Projects Agency Report, 28 October 1983.

2. Infrared and Optics Division, "Investigation of active/passive line scan techniques", Technical Report AFAL-TR-75-162, Environmental Research Institute of Michigan, Ann Arbor, Michigan, January 1976.

3. Infrared and Optics Division, "Investigation of Iso-range Contour Sensor Techniques: a Target Height Cueing Sensor", Technical Report AFAL-TR-75-212, Environmental Research Institute of Michigan, Ann Arbor, Michigan, July 1976.

4. Larrowe, V.L., "Operating Principles of Laser-Ranging, Image-Producing (3D) Sensors, Report 628109-1-X, Environmental Research Institute of Michigan, Ann Arbor, Michigan, December 1986.

5. Zuk, David M., and Dell-Eva, Mark L., "Three-Dimensional Vision System for the Adaptive Suspension Vehicle", Report Number 170400-3-F, Environmental Research Institute of Michigan, Ann Arbor, Michigan, January 1983.

These investigations utilized ERIM's tabletop 3D sensor to collect sample range data on model terrain scenes; the program culminated in a design study to outline the basic performance parameters and determine methods of hardware implementation for the vehicle's vision sensor.

In December 1982, under DARPA Order 4670, ERIM was awarded a contract (DAAE-07-83K-R008, issued by the US Army TACOM) for the fabrication of the vision sensor for the ASV. The sensor was delivered to OSU in mid-1984.

In 1984, under the same DARPA order, ERIM was funded to provide sensor support for the DARPA Autonomous Land Vehicle program (Contract DAAE07-84-K-R002). This document is a final technical report on that program.

The program provided for support in four primary areas:

1) Retrofit of the ASV sensor and support of the ASV sensor for FY 85-87.

2) Fabrication of additional 3-D sensors for DARPA ALV contractors.

3) Collection of 3D sensor data at the DARPA-Martin ALV test site near Denver, Colorado.

4) Design and fabrication of a multispectral ALV (MS-ALV) sensor for the DARPA Autonomous Land Vehicle.

This report is formatted such that a section is devoted to each of the above tasks.

SECTION 2
ASV SENSOR SUPPORT

ERIM designed and fabricated a 3D sensor as the vision sensor for Ohio State University's Adaptive Suspension Vehicle[6]. A photograph of the OSU "6-legged vehicle" is shown in Figure 1. The vision system delivered was a "brass board" sensor and was not extensively tested by ERIM prior to delivery. Figure 2 shows a photograph of the ASV sensor as initially delivered to OSU. At the time of delivery, ERIM was aware of several potential problems; specifically, scan motor overheating and retro-reflection of the laser diode energy from the sensor's front window. Therefore, as part of the current program, ERIM proposed to retrofit the sensor to correct these deficiencies; in addition, support was to be provided for the sensor through FY-87.

The sensor was returned to ERIM in July 1984 for installation on ERIM's instrumented van and was more thoroughly "wrung out" and subjected to vigorous field testing during a data collection exercise at the Martin-Marietta ALV test site near Denver, Colorado in September 1984. See Section 4.

---

6. Zuk, D.M., Dell-Eva, M.L., and Van Atta, P., "3D Sensor for Adaptive Suspension Vehicle", Report Number 164700-4-F, Environmental Research Institute of Michigan, Ann Arbor, Michigan, November 1984.

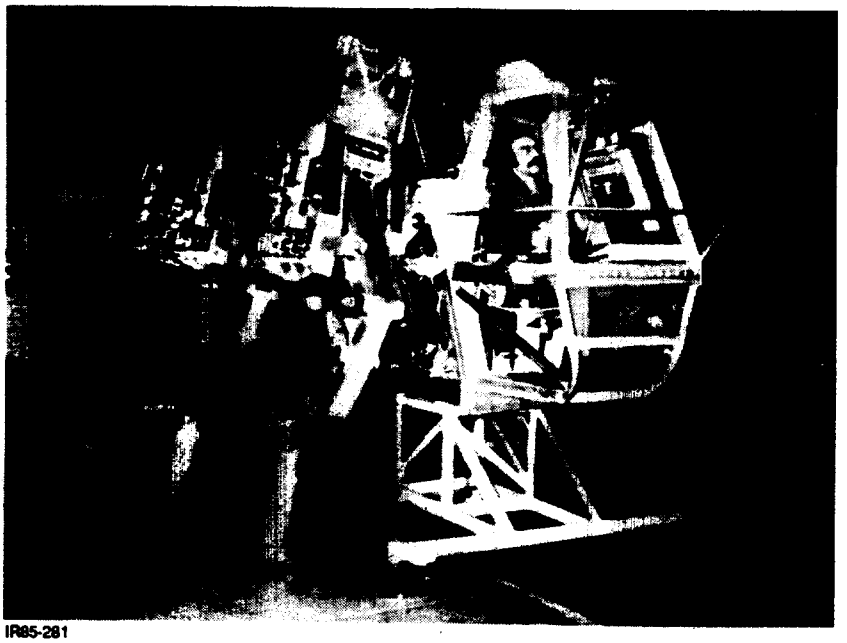

IR85-281

FIGURE 1. ADAPTIVE SUSPENSION VEHICLE

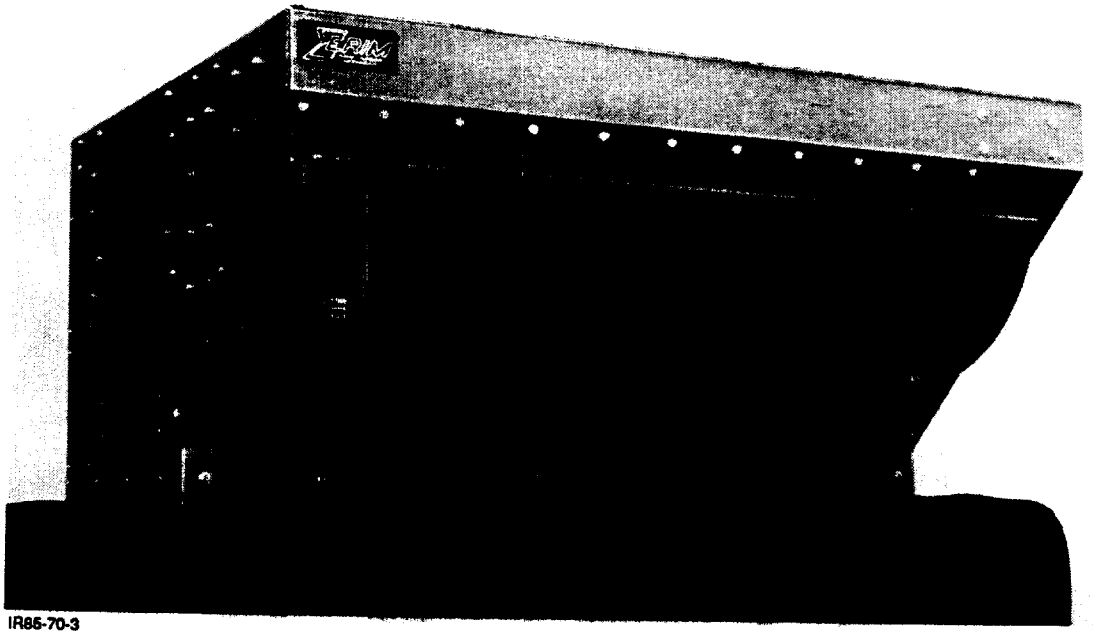

IR85-70-3

FIGURE 2. FRONT VIEW OF THE ASV SENSOR

2.1 ASV SENSOR RETROFIT

It was planned to carry out the retrofit of the sensor immediately after the data collection period in September 1984; in fact, parts were ordered for the sensor prior to deployment to Colorado. The re-design of the scan motor assembly provided for a more efficient motor and allowed the removal of bulky transformers and capacitors in the drive circuitry. Delays were encountered, however, when it was discovered that a new polygon scan mirror did not conform to specifications; the hole through the center of the mirror was not on axis and it had to be returned to the vendor and be rebored.

Retrofit delays also were encountered with the new sensor window which was to be fabricated of glass molded with a curved surface. The initial vendor withdrew his proposal at the last minute; a second vendor, under contract, had a fire in his plant and could not deliver, resulting in the cancellation of the purchase agreement. A third vendor was able to deliver a curved plastic window in December 1984. The window mounting was modified and the new window installed.

The sensor was returned to OSU in mid-January 1985 with the delays having no serious impact on the ASV program. Final testing indicated that residual heat build-up within the chassis was still possible and that it would be desirable to install ventilation fans at some future time.

2.2 ASV SENSOR SUPPORT, FY85-87

ERIM continued to support the ASV sensor throughout the contract period. Listed below are specific services performed during the program.

1) May 1985: The sensor was returned to ERIM for replacement of several op-amps believed damaged by voltage transients. A ventilated cover plate, to alleviate internal heat build-up, was also installed at this time.

2) Jan 1986: OSU requested ERIM field service to assess operating problems relating to scan mirror instability and low sensitivity. Recommendations were made for replacement of the laser diode (20mW) with a 100 mW unit.

3) May 1986: The ASV sensor was returned to ERIM for replacement of the laser diode and evaluation of the line synchronization problems. The latter problem was solved by using a sync phase-adjuster circuit to replace a portion of the original circuitry.

4) Feb 1987: The sensor was returned to ERIM to adjust amplifier gain. The higher power laser diode installed in May 1986 caused increased signal resulting in occasional amplifier saturation.

SECTION 3
ALV 3D SENSOR

The original contract provided for the fabrication of two additional 3-D sensors for ALV contractors, Martin-Marietta and Carnegie-Mellon University (CMU). A design study was performed at the onset of the program to identify specification changes from the ASV sensor that might be desirable for the new units. Table 1 lists the parameters for the new "ALV" sensor. Notations show how the parameters differ from the ASV sensor.

A contract modification was also effected in September 1985 for fabrication of a third ALV sensor for delivery to Sandia National Laboratories.

Delivery of the 3D sensors was made on the dates indicated below:

Martin Marietta	March 1985
Carnegie-Mellon University	May 1985
Sandia National Laboratory	January 1986

3.1 GENERAL DESCRIPTION OF THE ALV SENSOR

The ALV sensor was designed for the DARPA-Martin Autonomous Land Vehicle. Figure 3 depicts the vehicle traversing a roadway at the Martin-Denver test site. The sensor is located behind the window area at the top-front of the vehicle. Figure 4 provides a front view of the sensor.

A functional block diagram of the 3D sensor is presented in Figure 5. The 3D sensor's scanning mechanism directs the laser beam and the field of view of the detector to the scene. The modulator-driver provides a modulated signal to drive the diode laser and also a phase reference signal to the digital phase detector. The optical detector converts the

TABLE 1

ALV SENSOR PARAMETERS

TFOV	
Horizontal	80°
Vertical (1)	30°
IFOV (2)	0.5°
Beam Size	0.44 ft (at 50 ft)
Horizontal Pixels (3)	256
Vertical Lines	64
Ambiguity Interval (4)	64 ft.
Frame Rate	2 Hz
Data Rate	92160 Hz
Laser Power (5)	100 mW
Wavelength	0.82 μm
Range Noise	0.4 ft (at 50 ft, 10% refl.)
Output Signal	Analog-Logarithmic
Sensor Dimensions	
Height	14 in.
Width (6)	29 in.
Depth	22 in.
Weight	75 lbs.
Power	24 vdc, 300 W

(1) Reduced from 60° for ASV Sensor (Depression angle adjustable via external mount).
(2) Reduced from 1° for ASV Sensor
(3) Increased from 128 for ASV Sensor
(4) Increased from 32 ft. for ASV Sensor
(5) Increased from 20 mW for ASV Sensor
(6) Increased from 26 in. for ASV Sensor

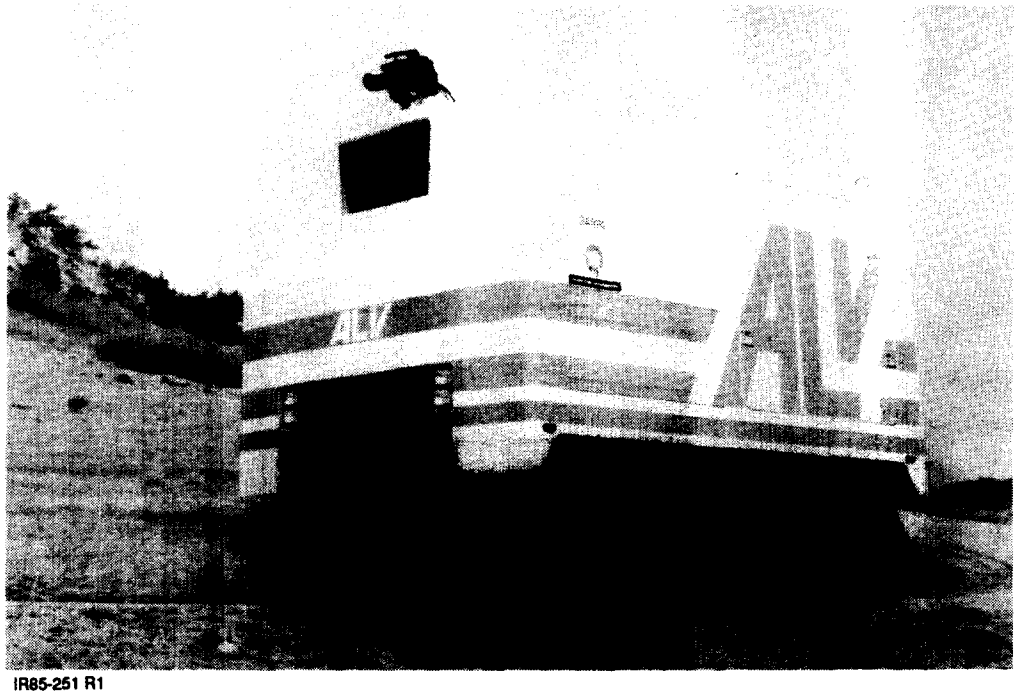

IR85-251 R1

FIGURE 3. DARPA-MARTIN AUTONOMOUS LAND VEHICLE

IR85-217-4

FIGURE 4. FRONT VIEW OF THE ALV SENSOR

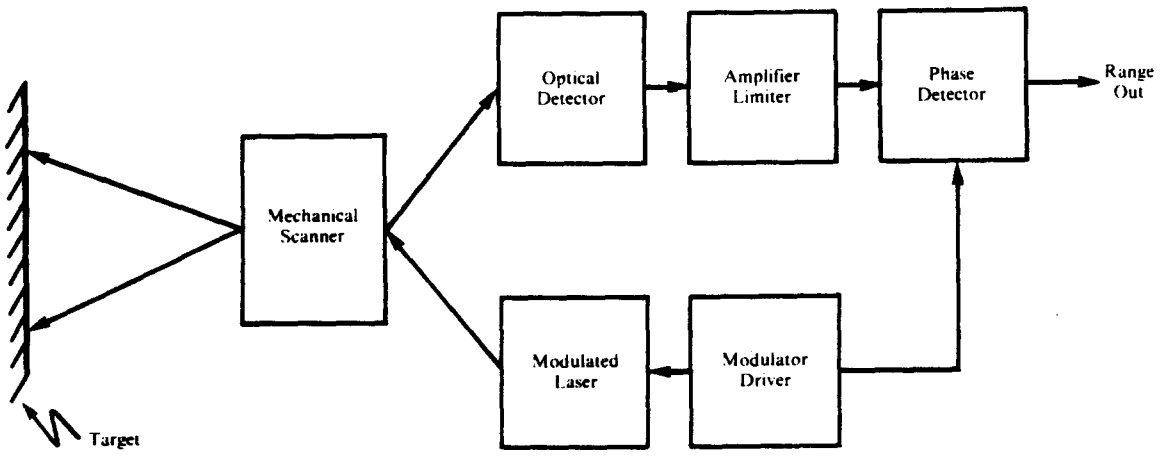

FIGURE 5. BLOCK DIAGRAM OF 3D SENSOR

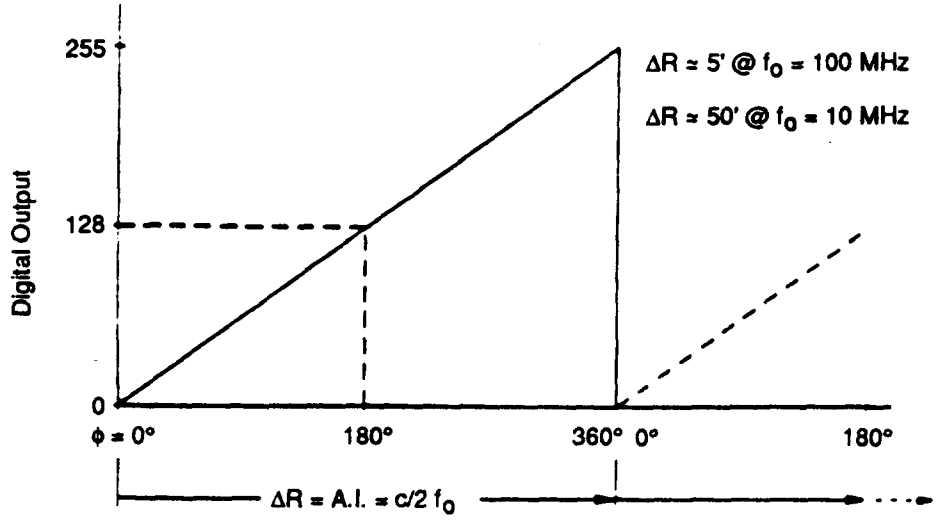

FIGURE 6. MODULATION FREQUENCY SENSITIVITY OF A DIGITAL PHASE DETECTOR

reflected modulated optical energy to an electrical signal whose ac component is amplified and limited. The limiting operation removes amplitude variation caused by the varying reflectance of the scene. The resulting signal, which contains phase but no amplitude information, is the second input to the phase detector. The output of the phase detector is a signal representing the phase difference between the reference and reflected signals, and corresponds to the range from the sensor to the target (for distances less than 64 ft.; for distance greater than 64 ft. the signal is modulo range). The amplitude signal is diverted and amplified without limiting, and recorded along with range data for every pixel.

The output of the digital phase detector is illustrated in Figure 6. The digital output value varies linearly according to the phase difference between the reflected return signal and the reference signal. The relationships between the ambiguity interval, the phase, and the modulation frequency are shown. Note:

- The ambiguity interval corresponds to a phase difference of 360 degrees.

- A 360 degree phase shift or an ambiguity interval is equal to $C/2f_m$ where C is the velocity of light and f_m is the modulation frequency.

The figure illustrates that half an ambiguity interval corresponds to a 180 degree phase shift which, in turn, is represented by a digital output of 128 from the digital phase detector. The distance represented by 128 depends upon the modulation frequency. If f_m is 100 MHz, then half the ambiguity interval (0.5 ΔR) represents 2.5 feet and, if f_m is 10 MHz, 0.5 ΔR is 25 feet.

A relatively simple relationship exists between signal-to-noise and the measured range noise. The signal-to-noise is represented by the equation:

$$(S/N)^2 = \frac{\langle i^2 \rangle_{sig}}{\langle i^2 \rangle_{noise}} \qquad (1)$$

where $(S/N)^2$ is the power signal-to-noise ratio
$\langle i^2 \rangle_{sig}$ is average of the square of the signal current
$\langle i^2 \rangle_{noise}$ is the average of the square of the noise current

When $(S/N)^2 \geq 30$, an approximation can be used to obtain the expression for range noise in terms of $(S/N)^2$.

$$\sigma_R = \frac{\Delta R}{2\pi} \cdot \frac{1}{\sqrt{2(S/N)^2}} \qquad (2)$$

where ΔR is the ambiguity interval and σ_R is the noise-equivalent range change or standard deviation. Complete independent derivation of this relationship can be found in Reference 2.

3.2 SUMMARY OF SENSOR OPERATION

The ALV sensor is basically a turnkey system. The operator control consists of an on-off switch and a pair of indicator lights. The first light comes on when the power is applied and the second light comes on when the laser diode interlocks are satisfied and the laser starts emitting.

When power is initially applied, a number of things must occur before the system can operate. When the power switch is thrown, the power relay is activated and the primary power is applied to the system. Initially one can expect a

startup current of from 12 to 15 amperes at about 28 volts DC. The current will pulse about 2 to 3 amperes twice a second as the nodding mirror snaps back to its starting position. The initial current surge will drop back to 9 to 11 amperes after 15 to 20 seconds. The current reduction occurs when the scan mirror comes up to speed and locks in sync.

There are four indicator lights that can be seen through the sensor window. The right-most light comes on if the laser diode is at the correct temperature. If it isn't, a thermoelectric cooler will either heat or cool the diode to the correct temperature. The second light from the right is energized when the nodding mirror is operating. The third light from the right comes on when the scan mirror is up to speed. The left-most light comes on when all the other lights are on and the interlock switch is in its proper position. When the left light is on, the laser diode is energized and the run light which is visible to the operator also comes on. When power is first applied, the laser diode starts "softly". The diode comes up to full power after about 10 seconds. The "soft" startup is recommended by the diode manufacturer.

The computer interface sends data to the computer. Data is loaded into a FIFO when the line sync indicates a new line has started and ends when the FIFO is full or a line (256 pixels) of data is sent. Both data and a line number are sent to the computer. The line number changes when a new line of data starts and any old unread data is cleared from the FIFO.

3.3 ALV SENSOR SUPPORT, FY 86-87.

ERIM provided limited support for the ALV Sensors through out the contract period. Specific services performed are discussed below:

1) Oct 1985: An ERIM field service engineer was sent to Carnegie Mellon University (CMU) to assess operating difficulties and provide instruction on the CMU sensor.

2) Jan 1986: ERIM engineers again visited CMU after inquiries regarding the operation and performance of their sensor. The jitter on the sensor video was considered excessive. Although this was partially remedied at CMU's facilities, a fundamental problem was determined to exist with all 3D sensors and hence the phase-lock-loop for the mirror drive was redesigned; modifications were subsequently incorporated in all ALV Sensors.

3) Mar 1986: An ERIM engineer responded to inquiries from the Sandia National Laboratories by an on-site visit. Adjustments were made in the synchronization circuitry of the sensor and recommendations were made regarding sensor interface.

4) Jun 1987: ERIM engineers visited Martin's facilities to correct the line jitter problem associated with their sensor. In addition, the 100mW Laser-Diode was replaced with a 200mW unit to

improve operating range. The optical system was realigned and proper performance of the sensor was verified.

5) Aug 1987: The Martin ALV Sensor was returned to ERIM for replacement of the Laser Diode which was determined to be defective.

(THIS PAGE INTENTIONALLY LEFT BLANK)

SECTION 4
DATA COLLECTION

The original ALV contract provided for two data acquisition periods at the Martin-Denver ALV test site. Because of the desire to obtain 3D data early in the program so that the vehicle contractor (Martin Marietta) and other vision contractors could have data for developing Vehicle Navigational Algorithms, arrangements were made to use the 3D sensor previously delivered to Ohio State University. ERIM installed the sensor on its instrumented van (see Figure 7) and deployed to the Martin-Denver site in September 1984. Considerable sensor data over various terrain types were generated and selected portions were reformatted to computer tapes, duplicated, and distributed to the ALV contractors.

The September 1984 acquisition period was considered to be the "dry" vegetation period. The subsequent measurement period was in July 1985 when "wet" or green vegetation prevailed at the Denver site. By this time ERIM had its own 3D sensor and that was used to perform the measurements since it had characteristics identical to the sensor intended for the ALV.

As the DARPA ALV program evolved it became apparent that there was also a need for multispectral data at the ALV Denver site. These data were needed to provide vision contractors with: (1) basic data which algorithms could be generated and tested and, (2) test data for ERIM to verify band selection for future cross-country navigation. ERIM proposed to modify a passive airborne multispectral (MS) scanner and mount it on its van for additional measurements. Note, Figure 6 shows both the ALV 3-D sensor and the MS sensor mounted on the pallet over the cab on ERIM's van. A

IR85-296-2

FIGURE 7. ERIM'S INSTRUMENTED VAN

separate contract (DAAE07-86-C-R019) was therefore negotiated for these additional measurements.

ERIM participated in four measurement periods altogether at the Denver site:

1) September 1984
2) July 1985
3) September 1985
4) May 1986

A final report[7] was written under the second contract which discusses in detail all measurements including details of instrumentation, calibration, data format, distribution of the data, and as appendices, the data collection logs.

7. Miller, C.D., "Image Sensor Data Base for the DARPA ALV Program", Report Number 193600-1-F, Environmental Research Institute of Michigan, Ann Arbor, Michigan, October 1986.

(THIS PAGE INTENTIONALLY LEFT BLANK)

SECTION 5
MULTISPECTRAL ALV SENSOR

The development of the multispectral ALV (MS-ALV) sensor was proposed as a three-year program with the first year devoted primarily to the sensor design study. Initial parameters desired for the sensor are indicated in Table 2.

TABLE 2.
PRELIMINARY SENSOR REQUIREMENTS

Operating Range:	0 to 100-200 ft.
Resolution:	X, Y, Z, Sufficient for Scene Characterization (6-12" nominal)
Frame Rate:	2 per second
Field of View:	Azimuth 40° Elevation 60-90°
Vehicle Velocity:	0-50 km/hr.
Meteorology:	Adverse Weather, Day-Night
Wavelength:	4-6 wavelengths of simultaneous operation

Considerable effort was devoted to selection of optimum wavelengths and subsequently the selection of laser sources with adequate power for those wavelengths. A preliminary design review for the sensor was held in June 1985, 11-months after contract inception, at which time all preliminary design results and the basis thereof were presented to the sponsor and members of the ALV community. Subsequent critical design reviews were held with the ALV vehicle integrator, Martin Marietta, and the sponsor in December 1985 and February 1986.

The following paragraphs describe the process used to define the specifications for the active multispectral sensor, lists the sensor's design parameters, provides a brief description of each sub-assembly and gives preliminary results of laboratory tests on the sensor.

5.1 BASIS FOR CONCEPTUAL DESIGN

An intelligent selection of spectral bands for an active system starts with a determination of desired classification distinctions. In the case of an autonomous vehicle, important classes relate to trafficability. Previous studies[8] have been performed which utilized passive multispectral data to access trafficability. Examination of the passive studies indicated that trafficability could be determined by examining vegetation and soil properties. The previous work was based on an existing sensor and the band selection was not necessarily optimum. Therefore, a study was initiated to determine spectral bands based on available information relating spectral regions to vegetation and soil properties.

The specific bands, i.e., wavelength regions, selected for the ALV multispectral scanner were obtained by combining information from three different sources: a computer modelling study, empirical data analysis and the Thematic

8. F. Thomson, R. Shuckman, K. Knorr, J. Ott, F. Sadlowski, "Studies of the Utility of Remotely Sensed Data for Making Mobility Estimates Using AMC Mobility Models", Report Number 14400300-2-F, NCSC Panama City, FL, November 1980.

Mapper (TM) tasseled cap transformation work [9,10]; these will be discussed individually below. Certain general conclusions arise from all three approaches: (1) for the purpose of scene analysis, bands can be placed in three spectral regions, visible, near infrared (NIR) and short-wave infrared (SWIR); (2) it is always advantageous to use bands in more than one spectral region and, for a variety of scenes, it is more important to have all spectral regions represented than any specific wavelength; (3) the value of a particular band is a function of the specific terrain types in the environment and (4) the marginal utility of each additional spectral band decreases.

The computer modelling study was undertaken to determine the number and wavelength range of spectral bands required to discriminate between representative examples of key terrain types for important environments. Details of the study may be found in [11]. Measured spectral reflectance curves covering the region of 0.4 to 2.6 μm were selected and classified/partitioned for particular terrain types and conditions. An example might be sandy loam under the conditions of a specific percentage of vegetation cover and a particular viewing angle. The spectral reflectance data

---

9. E.P. Crist and R.C. Cicone, "A Physically-Based Transformation of Thematic Mapper Data--The TM Tasseled Cap", IEEE Trans. Geo. Rem. Sens. GE-22, 256 (1984)

10. R.J. Kauth and G.S. Thomas, "The Tasseled Cap--A Graphic Description of the Spectral-Temporal Development of Agricultural Crops as Seen by Landsat", in Proc. the Symposium on Machine Processing of Remotely Sensed Data, Purdue University, West Lafayette, Indiana, 4B-41 (1976).

11. J. Colwell, "Simulation of Reflection Properties of Selected Terrain Features Under a Variety of Viewing Conditions", ERIM Technical Report, March 1985.

were broken into 153 spectral bands and the differences in these curves were analyzed to obtain a set of wavelengths which would maximize the potential for discrimination among the chosen terrain types. Table 3 presents the spectral bands selected by this method and the features for which each was found to be a valuable discriminant. This set of bands was subsequently reduced to a single band in each of three spectral regions. See Table 4. The 0.52 - 0.55μm band was not chosen since it was determined that water depth was not a major feature for measurements in the initial efforts. It should also be noted that the 1.65μm band provides equivalent feature measurement properties.

TABLE 3.

SUMMARY OF SPECTRAL BAND SELECTIONS BY SPECTRAL REGION

Vegetation Properties		Soil Properties		Water Properties	
Wavelength Region	Use	Wavelength Region	Use	Wavelength Region	Use
.52-.55 μm	Green Refl. Peak	.52-.55 μm	Soil Comp.	.52-.55 μm	Water Depth
.62-.69 μm	Soil/Veg. Discrimination Veg. Condition	.62-.69 μm	Soil Comp.; Effects of Vegetation	.80-1.20 μm	Surface Phenomena
.80-1.20 μm	Veg. Density; Veg. Type	.8-1.2 μm	Soil Moisture; Effects of Vegetation		
		1.5-1.75μm	Soil Moisture Soil Type		
2.0-2.35 μm	Vegetation Type/Moisture	2.0-2.35 μm	Soil Moisture/ Composition		

TABLE 4

COMPROMISE SET OF OPTIMUM SPECTRAL BANDS

Spectral Band	Wavelength (μm)
Visible	0.67
Near Infrared	1.06
Shortwave Infrared	1.65 and 2.20

In order to verify the computer modelling and band selection, an empirical study was undertaken; i.e., data collected with a passive multispectral scanner (MSS) were analyzed. These data were obtained at the ALV test site near Denver, Colorado on July 3, 1985. The data were collected in the early morning with the MSS sensor mounted on the ERIM vehicle so as to closely match the illumination and viewing characteristics of an active system. Three scenes were chosen as representative of the terrain. A number of key features, listed in Table 5, were identified in the scenes. For each scene, regions were selected corresponding to particular terrain features and "training sets" were developed by which to test the probability of correct recognition (POCR) of scene elements using particular bands or combinations of bands.

Six bands from the MSS sensor, which were in the computer model selected spectral regions, were chosen for analysis of the scenes. These bands were picked as being potentially obtainable with an active system and representative of the key spectral regions. The characteristics of the six bands are summarized in Table 6.

TABLE 5

TERRAIN TYPES PRESENT IN EACG SCENE OF THE DENVER MSS DATA

Terrain	Scene 12	Scene 14	Scene 41
Concrete			X
Dry Areas			X
Bare Soil	X	X	X
Bare Rock	X		
Dry Grass	X	X	
Green Grass	X	X	X
Meadow		X	
Snowberry	X	X	
Shrub		X	
Sagebrush	X		
Yucca	X		
Oak	X	X	X
Conifers	X	X	X

TABLE 6

SELECTED SPECTRAL BANDS OF MSS SENSOR

Channel	Wavelength (microns)	Dynamic Range (95%)	Standard Deviation of Dark Level	Type
2	.47 - .54	39 - 152	1.6	Visible(green)
5	.62 - .66	35 - 141	1.0	Visible (red)
8	.77 - .86	35 - 215	2.5	NIR
10	1.0 - 1.4	37 - 170	6.0	NIR
11	1.5 - 1.8	44 - 204	4.2	SWIR
12	2.0 - 2.6	39 - 189	4.9	SWIR

The standard deviation of the dark level was calculated from a set of points in the vehicle's shadow in each scene and is included as an indication of the noise level inherent in each channel. As can be seen from column 4, the noise levels of the two SWIR bands are 2 to 3 times higher than the remaining bands. Optimal sets of bands were obtained for each scene by finding a single band with the maximum POCR, finding the combination of this band with a second which maximizes the POCR and so on, up to the combination of all 11 bands available from the MSS scanner.

The results of this procedure are shown graphically in Figure 8. On the horizontal axis, at the bottom, are listed the bands in order of selection using scene 12; above are listed the bands (in order of selection) from scene 41. In each case, a visible band was picked as the best single band but the particular band chosen was scene-dependent. For scene 12, band 5 (red) was the best single band while for scenes 14 and 41, band 2 (green) was chosen first. On the vertical axis, the probability of correct recognition of the training sets in each scene is plotted, in the range from 0.5 to 1.0. As can be seen from the figure, even a single band yields greater than 60% probability of correct classification of scene elements. The addition of a near IR band to the first visible band increases the POCR to above 85%. The third band chosen is always a SWIR band and only increases the POCR by about 5%. The relative values of the two near IR and the two SWIR bands were assessed as shown in Table 7. It can be seen from these results that the two near IR bands are nearly equivalent, as are the two SWIR bands.

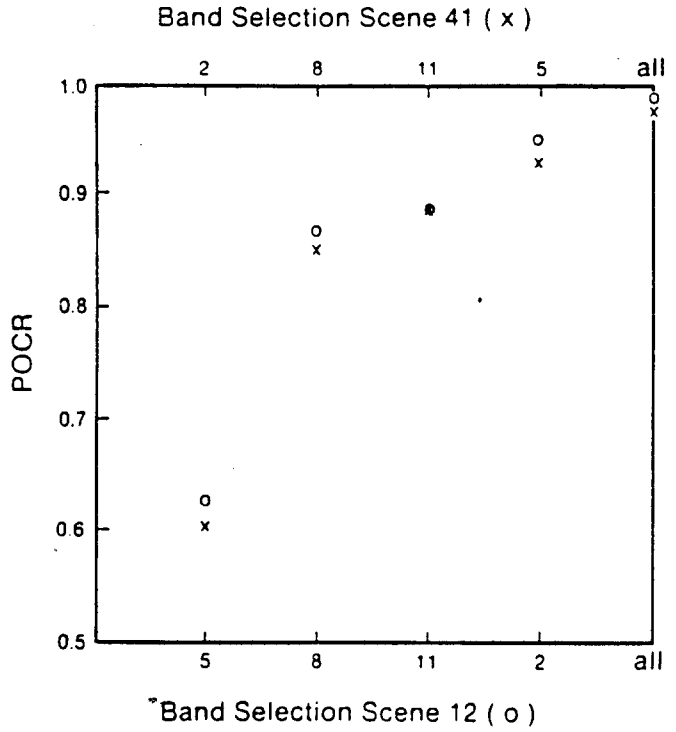

The POCR is plotted on the vertical axis as a function of the set of bands employed. On the horizontal axes are shown the order in which bands were selected for two scenes, 12 (bottom, circles) and 41 (top, triangles). Each point represents the POCR obtained for that scene using the indicated band together with all bands to the left on the horizontal axis.

FIGURE 8. POCR AS A FUNCTION OF BAND SELECTION

TABLE 7

POCR FOR REGION RESTRICTED SPECTRAL BAND SELECTION

	Band Combination			
Scene	2,5,8,11	2,5,8,12	2,5,10,11	2,5,10,12
12	.97	.95	.95	.97
14	.94	.90	.91	.91
41	.93	.93	.90	.93

These results suggest that the SWIR bands add little to the probability of recognition of terrain features. On the other hand, the role of the SWIR bands in the computer modelling study was primarily in identification of moisture, either of vegetation or soils. It is therefore possible that the Denver test site in July was too dry to adequately demonstrate the utility of these bands. As an additional source of empirical data, reported analyses of Thematic Mapper data from Landsat-4[9] were examined. In this work the authors developed a new Tasseled Cap[10] feature termed "Wetness" which is obtained from the difference of a weighted sum of the visible and near IR bands and a weighted sum of the SWIR bands. They demonstrated that this feature, when coupled with the brightness feature (a measure of total reflectance), allowed for clear separation of different soil types on the basis of moisture content. From this it was concluded that a SWIR band was indeed important for classification of a wide range of scenes although of limited value at the Denver ALV test site.

5.2 SENSOR DESIGN

The ALV multispectral sensor utilizes a scan mechanism similar to that employed in the ERIM designed ALV 3-D sensor (Section 3). The sensor utilizes a spinning polygon and nodding mirror as illustrated in Figure 9. This design uses adjacent faces of a hexagon scan mirror for the transmitted laser beam and receiver aperture. Using adjacent mirror faces enables one to use the largest aperture for both the transmitted and received beams. The large transmit beam enhances laser safety and the large receive aperture is required to obtain sufficient signal-to-noise to operate at longer ranges.

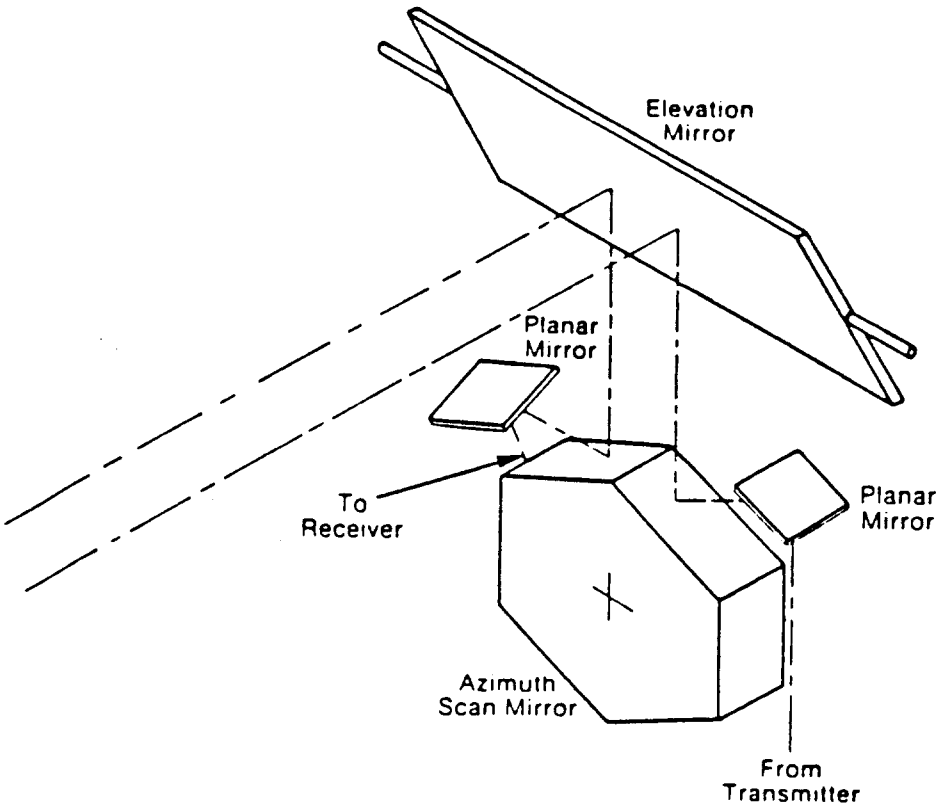

FIGURE 9. SCANNER OPTICS

The ALV multispectral sensor parameters are summarized in Table 8. There are 256 scan lines covering a 60° vertical field of view. The vertical field of regard of +30° to -50° depression angle is obtained with a 0 to 20° tilt adjustment. The horizontal field of view is 60° with 256 pixels per scan line. With a pan of ±45°, the horizontal field of regard is 75° to either side of the center line. The instantaneous field of view is 0.23 deg or 4.1 milliradians, corresponding to a 0.31 meter footprint at 75 meters (12 inches at 246 feet). Two 256 line by 256 pixel frames are collected per second. The combination of two modulation frequencies, 100 and 2 MHz, provides range resolution of 2 cm and an ambiguity interval of 75m. The data or pixel rate for each spectral band is 328125 Hz, with an information bandwidth of 164062 Hz. This corresponds to a line rate of 650.87 lines per second. The sensor is designed for a maximum of 7 spectral channels. Of these, three will be incorporated initially, with at least two more to be added at a later date.

TABLE 8

MS-ALV SENSOR PARAMETERS

Verticle FOV:	60° (256 scan lines)
FOR:	+30° to - 50° depression angle
Horizontal FOV:	60° (256 pixels per scan line)
FOR:	±75° from center line
:	±45° pan
IFOV:	0.23° or (4.1 mr)
:	0.31 meters at 75 meters (12 inches at 246 ft.)
Frame rate:	2 per second (256 line x 256 pixel frame)
Ambiguity interval:	75 m
Range resolution:	2 cm
Spectral bands:	7
Data/pixel rate:	328125 Hz per band
Information bandwidth:	164062 Hz per band
Line rate:	640.87 lines per second
Mirror speed:	106.8 rps or 6408.7 rpm

5.2.1 SOURCE

On the basis of the studies discussed in Section 5.1 a set of band priorities was established: visible > near infrared > short-wave infrared. The visible and near infrared bands were determined to be of primary importance for initial development at the Martin Denver test site. In order to obtain representation in these two bands with a minimum of laser sources, a mode-locked Nd:YAG laser with an extra-cavity frequency doubler (Quantronix Model 416-MLSH) was selected as a primary source of 1.06 μm (near IR) and 0.53 μm (visible, green) radiation. A laser diode (0.83 μm) was included as a backup to the 1.06 μm band.

For the addition of a second visible band and a SWIR band, Raman-shifting of both the 0.53 μm and 1.06 μm Nd:YAG wavelengths was investigated. The requirement of high repetition rates (MHz) precluded the use of a Q-switched pump laser for high peak powers. Instead, an alternative technique was explored utilizing the mode-locked Nd:YAG pump for moderate peak powers and a liquid scattering medium contained in a hollow silica capillary. With a scattering medium of higher refractive index than fused silica, the capillary acts as a waveguide for both the pump and the Stokes beams. Containing the laser beam in a capillary serves two functions: (1) to increase pump power density and (2), to increase the effective interaction length. By this means, the power requirement to reach the stimulated Raman scattering threshold can be reduced to levels achievable with a mode-locked source[12].

A material with a Raman shift of approximately 3000 cm^{-1} would serve to convert 0.53 to 0.63 microns and 1.06 to 1.55 microns, which would provide both red and SWIR wavelengths as desired. Dimethyl sulfoxide (DMSO), was selected as the scattering medium because it is known to have a large Raman scattering coefficient with a shift of 2916 cm^{-1} [13], it is transparent in the visible, near and shortwave infrared

regions and it is chemically inert and relatively non-toxic. The reported refractive index of DMSO is higher than fused silica over the wavelength range of interest, although the index difference is small (0.02-0.04) [14]. Hollow silica fibers of 25 and 100 micron diameters and lengths ranging from 0.3 to 1.5 meters were employed.

Stimulated Raman scattering at 0.63 microns was observed with 350 mW average mode-locked pump power at 0.53 microns, but was found to be only marginally above threshold. Further investigations showed that the interaction of the pump beam with the DMSO induces a strong thermal lens. Thermal lensing causes a reduction in refractive index of the DMSO. Because the refractive index of DMSO is initially only slightly higher than silica, this index reduction is sufficient to allow the pump radiation to couple out of the silica fiber and prevent efficient conversion of the pump beam to the Stokes wavelength. Experiments at 1.06 microns demonstrated that the pump beam couples out of the fiber before any conversion takes place.

---

12. A.R. Chraplyvy and T.J. Bridges "Infrared generation by means of multiple-order stimulated Raman scattering in CCl_4- and $CBrCl_3$- filled hollow silica fibers", Optics Letters 6, 632 (1981).

13. T.J. Bridges, A.R. Chraplyvy, J.G. Bergman, Jr., and R.M. Hart "Broadband infrared generation in liquid-bromine-core optical fibers", Optics Letters 7, 566 (1982).

14. C.D. Decker and P.J. Garner, "Efficient Raman/dye laser radiation source", Technical Report AFAL-TR-78-58 (1978); C.D. Decker, "High-efficiency stimulated raman scattering/ dye radiation source", Appl.Phys.Letter 33, 323 (1978).

As a consequence, alternative methods of frequency-shifting for the ALV multispectral scanner were investigated. Of these, the most feasible are the use of synchronously pumped dye laser, pumped by the doubled Nd:YAG at 0.53 microns for the red band and an F-center laser pumped by the 1.06 micron Nd:YAG fundamental to provide a band in the SWIR region. The source module for the ALV scanner has been designed so that these lasers can be incorporated in stages as the need for each is demonstrated.

A diagram of the source pallet for the MS-ALV Sensor is shown in Figure 10. The design utilizes the Nd:YAG laser as the fundamental source for the sensor. A GaAs laser diode is included to provide a low power backup capability. Energy from the YAG laser will be converted to other wavelengths for the other sources. The source pallet produce a single 4 mr diverging beam made up of the 5 source wavelengths.

The 1.06 μm laser beam and all of the laser beams derived from the 1.06 μm source have provisions for monitoring laser power. The small power fluctuations that exist in the 1.06 μm laser beam must be corrected if reflectance values are to be calculated to the desired accuracy.

Each of the separate wavelengths employ their own beam expansion telescopes. Separate telescopes are used so that chromatic aberations can be eliminated. The separate beams are combined into a single beam by using a series of mirrors and dichroic beam splitters. See Figure 10 illustration.

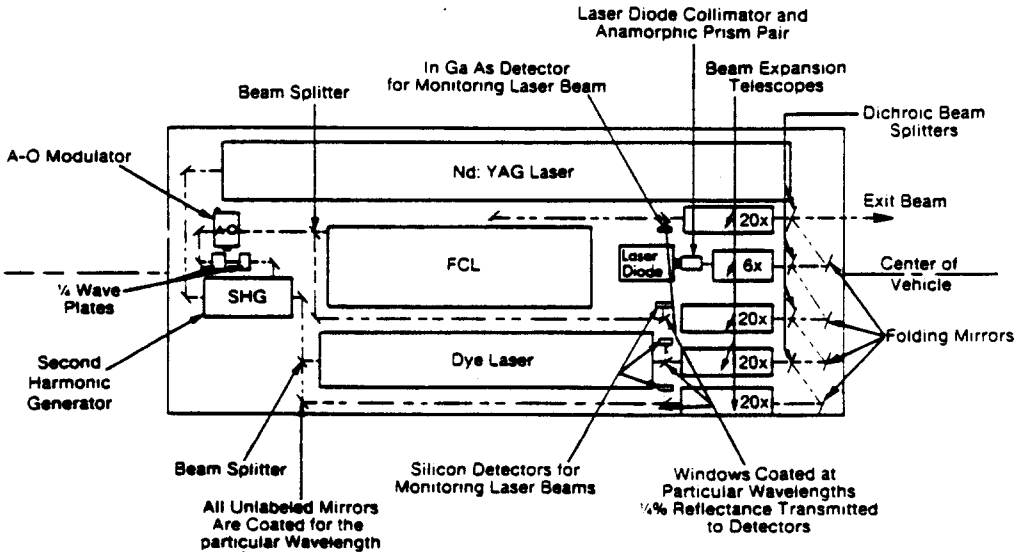

FIGURE 10. TRANSMITTER PALLET - DYE/FCL SYSTEM

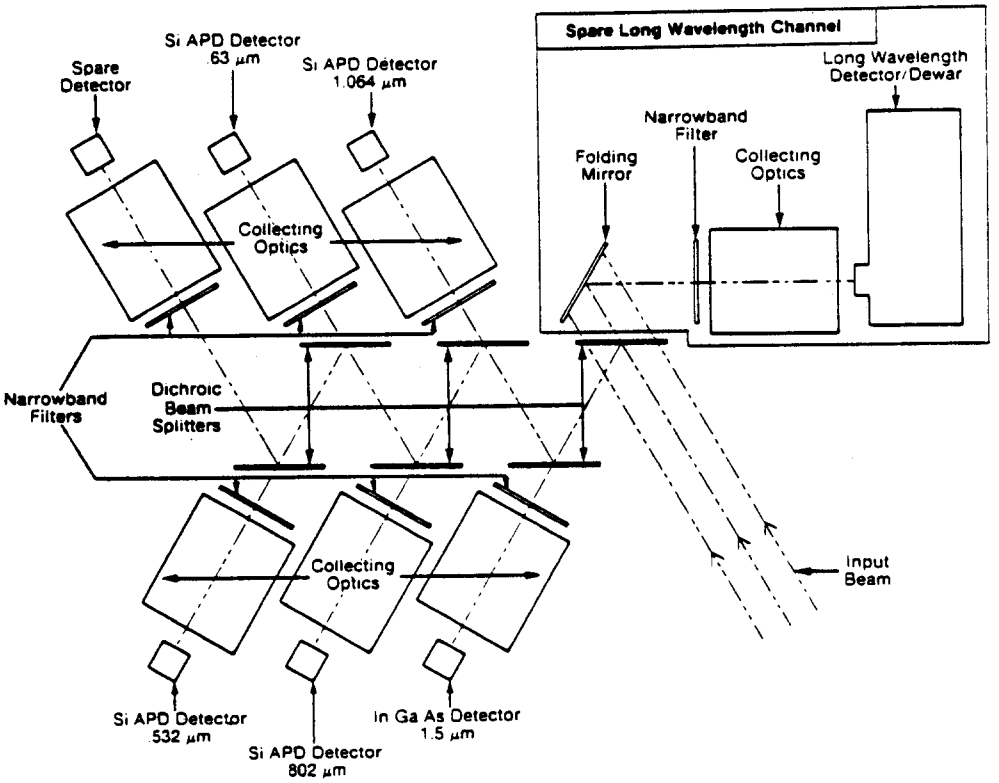

Figure 11. RECEIVER LAYOUT

5.2.2 RECEIVER

The receiver layout is illustrated in Figure 11. The input beam is separated into the various bands by a series of dichroic beam splitters. Each of the dichroics is a long-pass filter with high reflectance for shorter wavelengths. The spectral bands are further defined by narrow band interference filters in front of each lens. Each lens is coated for minimum reflectance at the wavelength of interest and is a multi-element assembly with low spherical aberrations.

Provisions have been made for seven spectral channels. Silicon Avalanche Photo Diodes (SiAPD's) are used for the four short wavelength bands. An InGaAs detector is used for the 1.5μm band and provision is made for a long wavelength channel plus a spare short wavelength channel.

5.2.3 ELECTRONICS

A schematic of the signal detection electronics is presented in figure 12. The signal from each detector goes through its own preamplifier before going to the RF detection electronics. The 1.06 μm channel also has electronics which generate the range measurements for the 3D image. The RF detector electronics consist of a narrow band filter which defines the Noise Equivalent bandwidth of the system, a logarithmic amplifier/detector and a A/D converter. The range electronics consist of the narrow band filter, a limiter to remove the amplitude modulated portion of the signal, and a digital phase detector. The outputs are multiplexed together and sent to the calibration electronics.

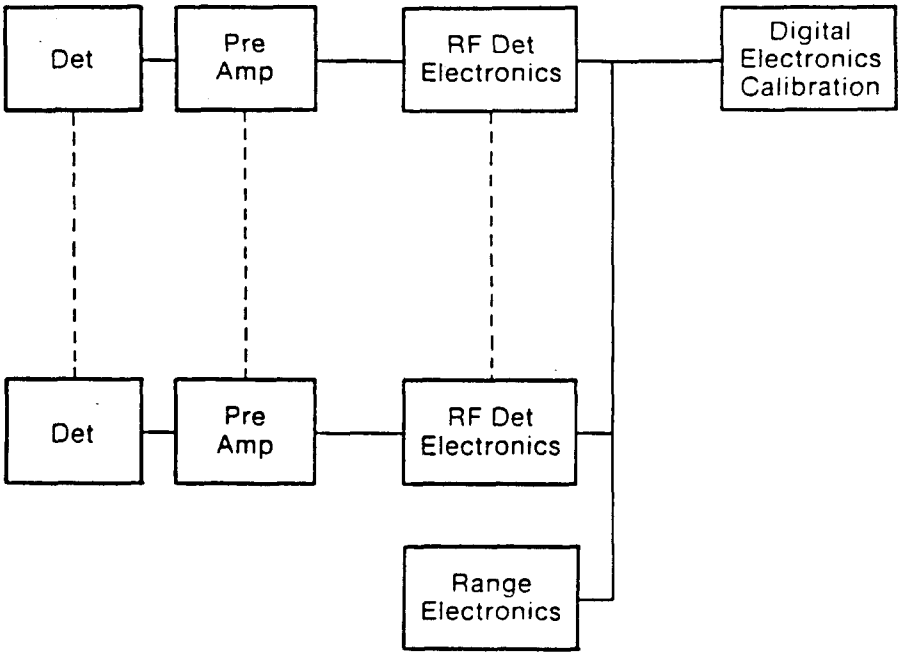

FIGURE 12. SIGNAL DETECTION ELECTRONICS

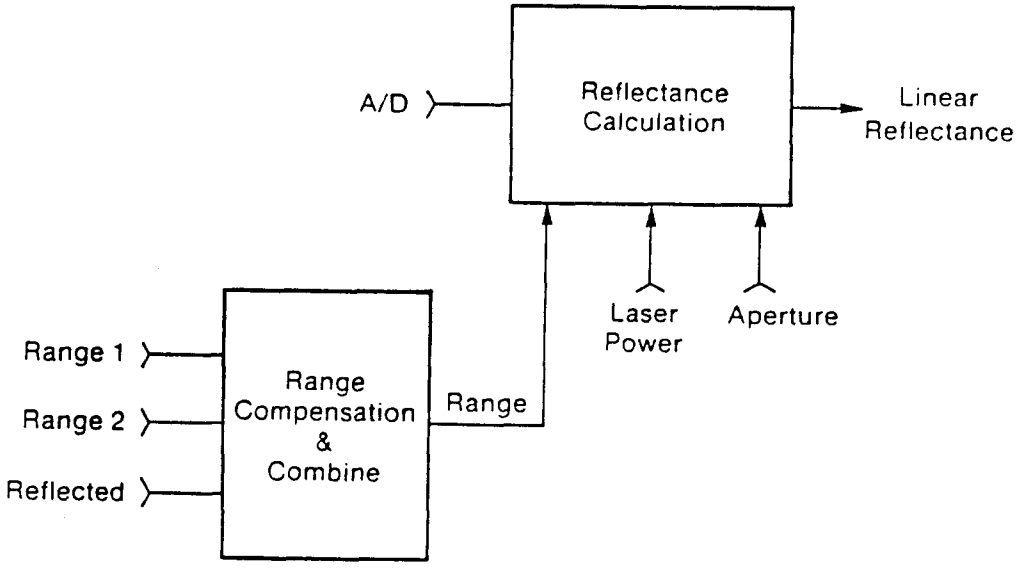

FIGURE 13. REFLECTANCE CALIBRATION CIRCUIT

5.2.4 CALIBRATION

The range measurements must be corrected for laser drift and reflected signal level. The range calibration takes place in the first block of Figure 13. The reflected signal for each pixel is used to correct for AM/PM conversion in the limiter and an internal range reference corrects for drift in the electronics.

The calculation of reflectance depends upon the response of the logarithmic detectors, the range calibration electronics, the laser power monitor, and the aperture function. The first correction performed is the linearization of the logarithmic response of the log amplifiers. Log amps typically have a 1 or 2 dB error over their dynamic range. Range data is inputted next so that the signal level change due to range is removed. Laser power fluctuations are corrected for by dividing by the laser power. An additional correction is included to compensate for the aperture function of the sensor. The aperture function arises from the change in the angle of incidence on the moving mirrors and window which make up the scanning mechanism of the sensor.

The resulting sensor provides calibrated multispectral reflectance and range data. The calculated performance of the sensor design is presented in Table 9. The limited range capability of the 1.53 μm channel is not a major concern even though this channel has the greatest impact on assessment of soils and soil moisture. Since the sensor will not usually be able to "see" the soils at the longer ranges due to vegetative cover (masking), soil moisture will have to be assessed at steeper look angles which imply short ranges. Availability of a stronger source and/or a more sensitive detector would permit longer range operation in limited situations where soil is relatively clear of cover.

TABLE 9

CALCULATED SENSOR PERFORMANCE

$\lambda(\mu m)$	$NE\Delta\rho$	Power (W)	Maximum Range For Specified $NE\Delta\rho$ (m)
0.53	0.002	0.3	46
0.63	0.003	0.1	38
0.82	0.003	0.1	34
1.06	0.004	1.0	76
1.53	0.010	0.15	14

5.2.5 MECHANICAL DESIGN

The MS-ALV sensor frame was designed to maintain the alignment of the transmitter and receiver systems to 0.1 of an IFOV or approximately 0.4 milliradians. Both the transmitter and receiver were designed as separate modules which could be modified separately as required. Separate modules facilitate modifying the transmitter when diode-pumped lasers or other state-of-the-art components became available. The frame was designed to keep the transmitter and receiver modules in alignment while experiencing up to 1g acceleration in any direction; the frame would not deform with up to 10g's of acceleration. In order to maintain alignment, it was necessary to keep deflections to less than 0.05 inches over a lever arm of 120 inches.

The transmitter was fabricated on a standard optical bench which consisted of a honeycomb structure that was laminated between two flat plates. The optical bench was choosen based on the rigidity it offered and the flexibility of changing the optical configuration of the transmitter. The rigidity of the optical bench maintains the alignment between the sources. Since the bench provides the rigidity

required to maintain alignment, the mounts for the optical components could be simpler and less expensive.

The receiver was fabricated on a single machined aluminum plate. A honeycomb structure was not used for the receiver because the necessary rigidity could be obtained with the plate. The single plate allowed adjustments to be traded for improved machining tolerances. For example, the structure that held the dichroic beam splitters was machined to a tolerance of less than +/- 0.001 inch which enabled the elimination of angular alignment adjustments for each dichroic beam splitter.

5.3 PRELIMINARY TESTS OF THE MS-ALV SENSOR

The fabrication of the main components of the MS-ALV sensor have been completed. Fabrication of some selected sensor items was deferred to allow for limited testing of the sensor; in particular, dust covers and some interconnect wiring was deferred. Fabrication of the various electronic subassemblies is complete, although detailed testing of some of these assemblies remains. Figure 14 shows the scan head assembly mated to the transmitter pallet. Figure 15 shows a rear view of the scan assembly with receiver optics and detectors mounted.

Preliminary testing concentrated on those portions of the system that are the most critical to the successful operation of the completed sensor. Since sensor deficiencies are hardest to correct if they occur in the source or receiver, the choice was made to collect images at ranges achievable in the laboratory; this would provide a good indication of how the sensor would operate when completed.

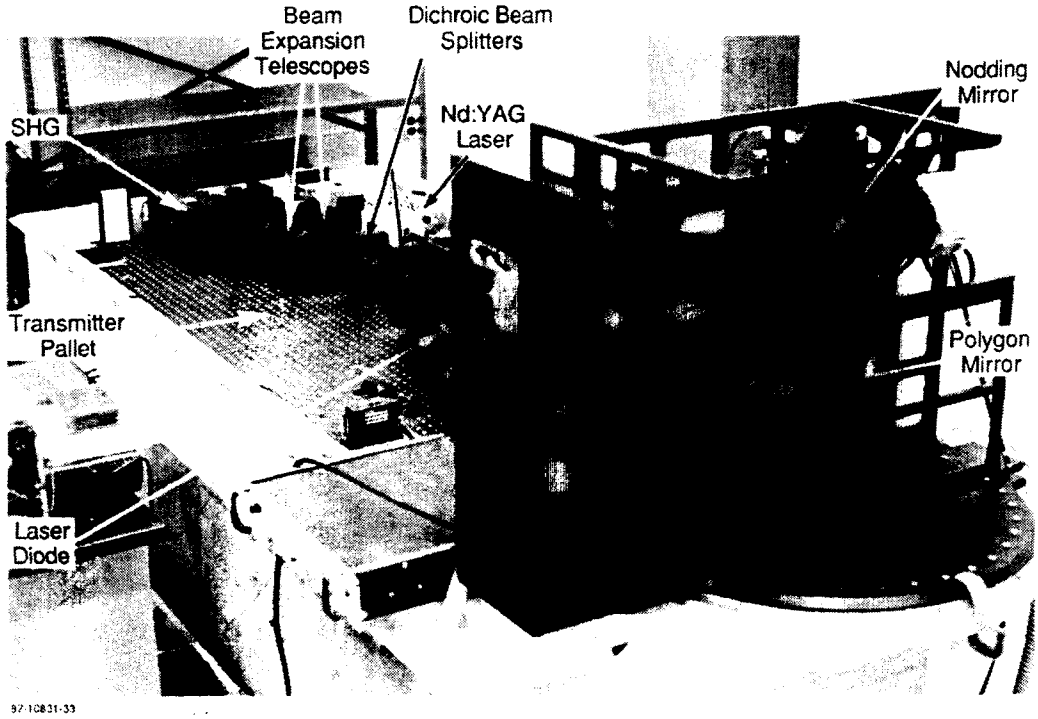

FIGURE 14. MS-ALV SCANNER AND TRANSMITTER PALLET

FIGURE 15. REAR VIEW OF THE MS-ALV SCANNING ASSEMBLY

Laser safety became a consideration in preliminary testing because the scan rate of the laser had to be slowed down to accommodate the data logging system being used to record/document test data. The test plan provided for collection of data with targets set at near ranges in the laboratory; subsequently, a first-surface mirror was used to extend the visible range through a window to an outside courtyard. The courtyard was chosen to circumvent problems with laser safety and to provide an outside as well as an extended range view. Figure 16 shows a plan view of the laboratory test scene.

The MS-ALV Sensor was operated from laboratory power. Laser cooling requirements were satisfied by a closed-cycle cooler that was available at ERIM's facilities. The speed control for the scan and the nod mirrors was not used as the scan rates required by the data logger were out of range for proper operation of the control circuitry. The transmit and receive assemblies are those that will be used in the final system. Substitutions were made in the electronics, ie, through the use of ERIM's 3D sensor, to facilitate data collection.

The reduced scan rates were a concession that was required by the use of the available data logging system. The data logger used is based on an IBM PC which sets a limit on the maximum data rate. The reduced data rate required that the scan mirrors be operated at a very slow rate to obtain image data. Digital data was stored on disk for subsequent data analysis and display.

Receiver alignment went as expected. The alignment of the receivers was performed twice on the system. Once at very short ranges available in the sensor laboratory and again at a longer range with the laboratory doors opened. The alignment proved that the adjustments worked well and as expected. The signals changed as expected as the system was intentionally misaligned. The tests also indicated that the adjustments are independent and orthoginal.

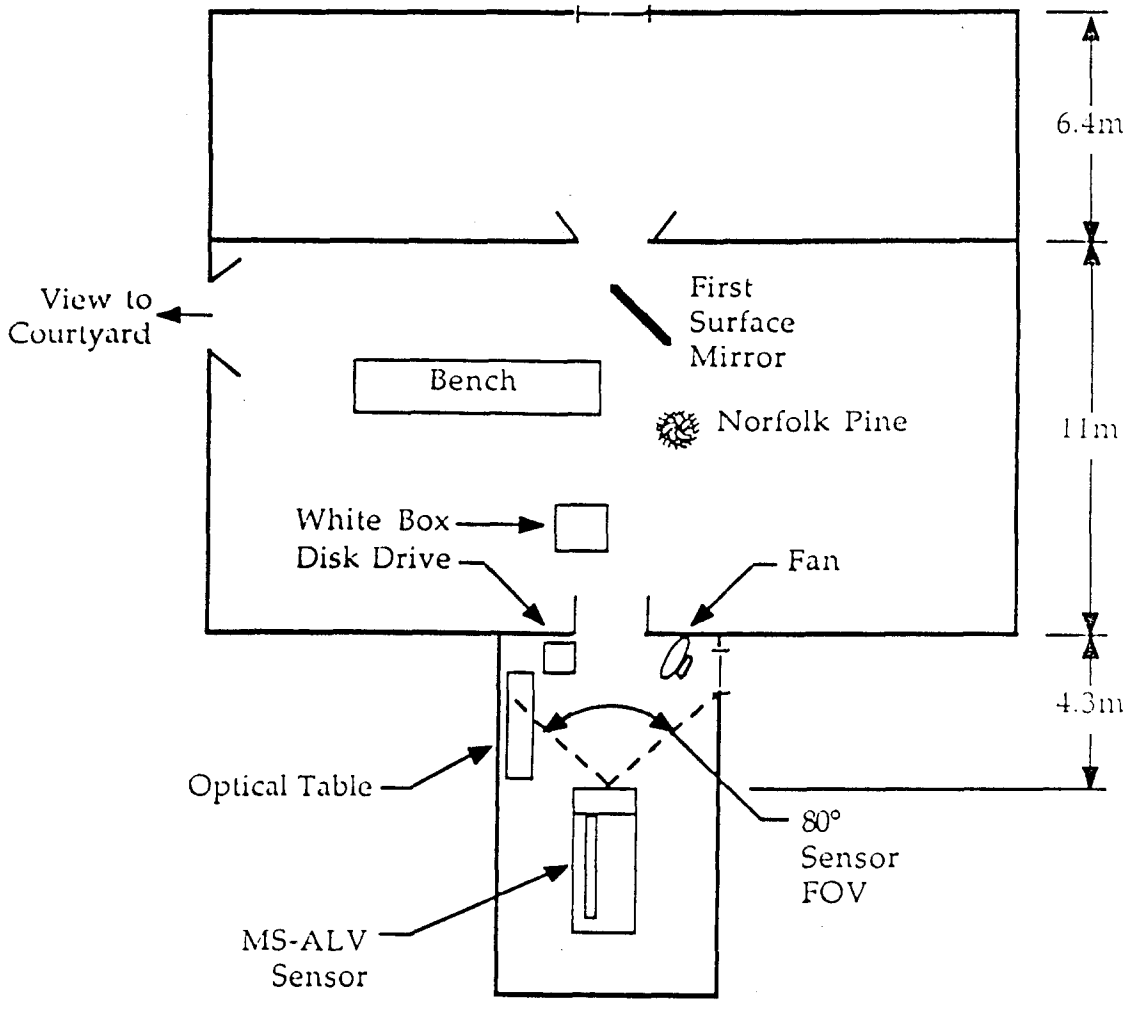

FIGURE 16. PLAN VIEW OF LABORATORY TEST SCENE

Data was collected with all three sources, ie, 1.06μm, 0.82 μm, and 0.53 μm, operating in conjunction with the corresponding three receiver channels. All three-channels were collected simultaneously and in registration. Data were recorded and saved on magnetic disks. Recorded data consists of three channels of reflectance and one of range.

A first order analysis of the data collected is presented in the following paragraphs. Measured performance is compared to the calculated performance of the sensor.

Figure 17 and Figure 18 are photographs of a CRT displaying images of all four data channels simultaneously. The upper left image is the reflected return data of the 0.53μm channel. The upper right is the 0.82μm (0.802 μm measured) reflected return. The lower left is reflected return of the 1.06μm channel. The lower right is the range data. The FOV of the sensor was adjusted to approximately 80^{o} horizontal by 35^{o} vertical with a 256 x 256 pixel resolution. The grey scale resolution was also 256. The bottom of the lower two images is truncated because the CRT was not able to display all 512 lines. The images in Figure 17 were taken with the receiver in alignment at long ranges and in Figure 18 at short ranges.

In order to assess the range performance of the sensor, data from the object at the farthest distance from the sensor were analyzed. The maximum range was extended to 63 meters by deflecting a portion of the sensors FOV with a first-surface mirror out a window onto a building across an outside courtyard. In Figure 17 the building can be seen in the center of the each image. In the reflectance data it appears as a rectangle with two bands of black on the top and bottom surrounding a wider band of grey in the middle. The dark bands are the brown brick veneer above and below the windows in the building. The windows appear lighter and as a grey tone because light-blue shades cover the windows on the interior. Calculations were made based on estimated

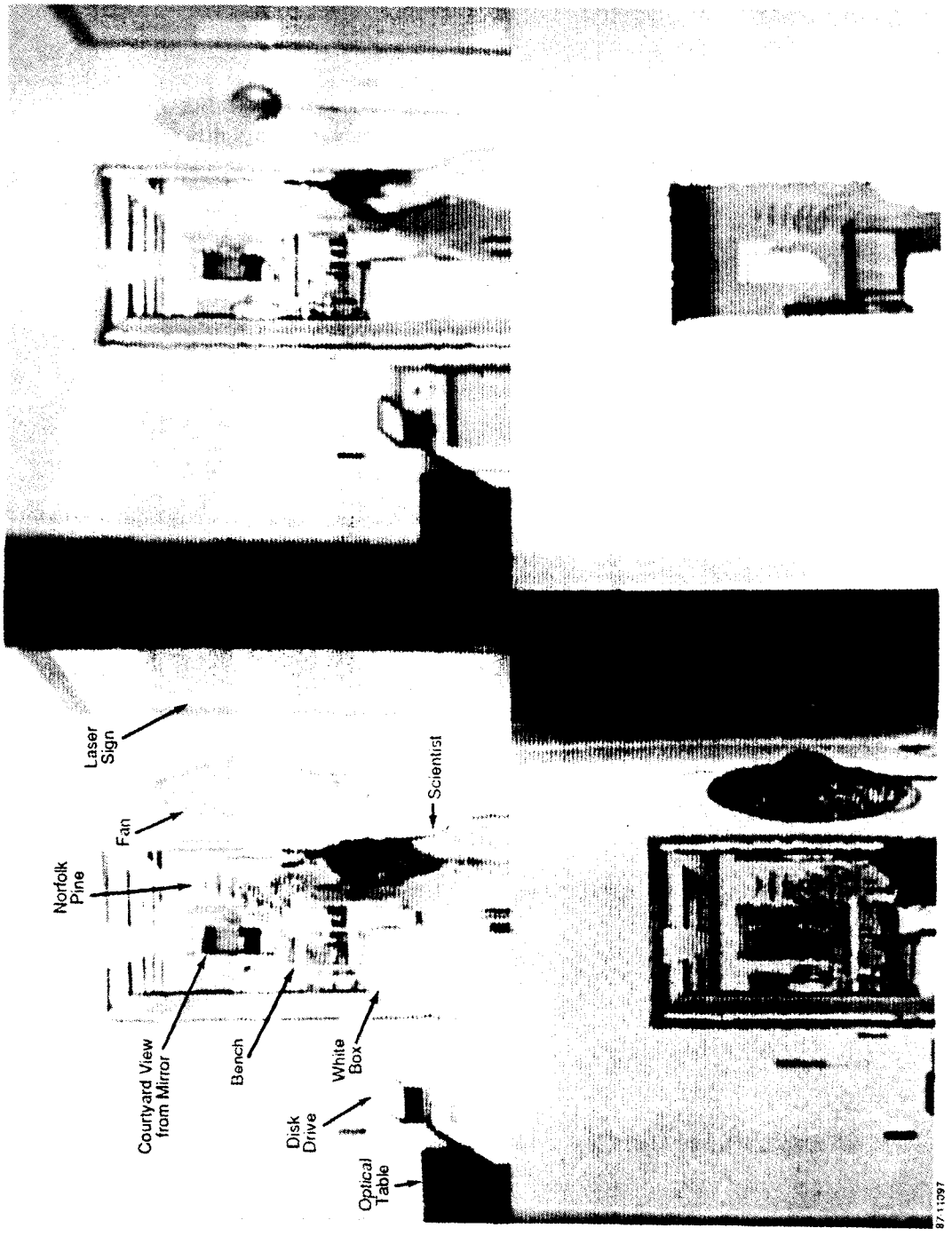

FIGURE 17. MS-ALV IMAGES AT SHORT RANGE

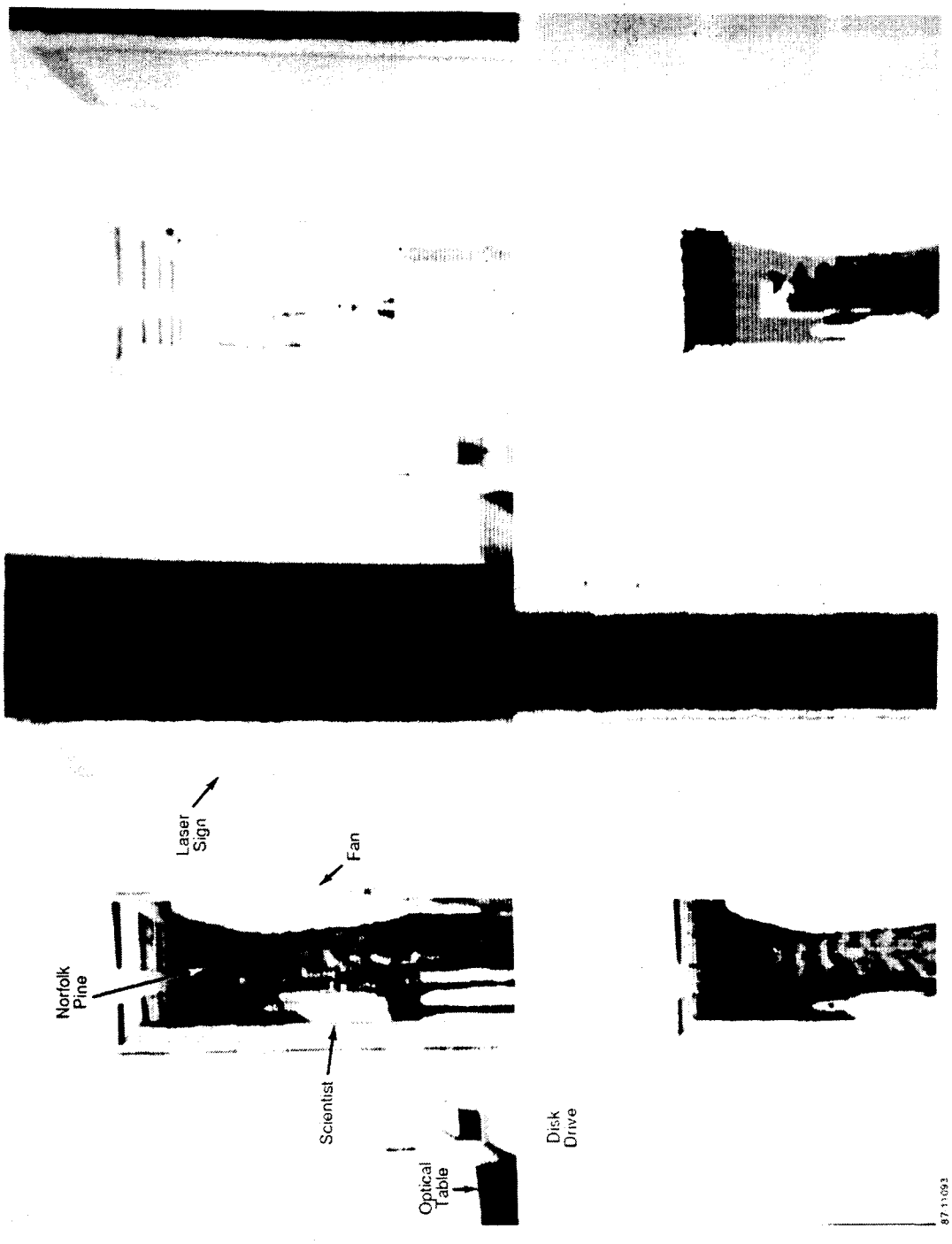

FIGURE 18. MS-ALV IMAGES AT LONG RANGE

sensor operating parameters at the time the data was collected. The calculated range resolution was 5.6cm. The data indicated a range resolution of 6.9cm at the maximum range. The discrepancy between the two is well within the bounds of calculation error in the approximations made for the parameters of the sensor. The close correlation between the calculated and actual performance indicates that the sensor is operating as expected.

The preliminary data also reveals the discriminatory nature of the multispectral information. A Norfolk pine was placed in the sensor FOV for this purpose. In Figure 17 the pine is located in the background just to the right of center. The spectral dependence of the reflectance of the foliage is readily observed in the raw data. The foliage is notably brighter in the near IR than in the green. Spectral discrimination of other objects in the scene are also evident. The dyes in the lettering on a laser warning sign fastened to a door on the right are less visible in the IR than in the green. In Figure 18, the slacks of one of the scientists in the lab show up brightly in the IR and appear dark in the green. Differences can also be seen in the brightness of human flesh, wood, and other articles in the FOV. The contrast observed between the three spectral bands in this preliminary data set confirm that the multispectral feature of the sensor has discriminatory capabilities.

The performance characteristics as calculated from laboratory parameters are presented in Table 10. Note, this should be compared with values in Table 9. A rigorous evaluation of the performance of the reflectance channels was limited by the 8 bits of resolution used in the data collection. The reduced resolution was a compromise that was made with scan rate for the available data logging system. In the 8 bit system, one count corresponded to a $\Delta\rho$ of approximately 0.05. With such resolution it was not possible to test for the goal $NE\Delta\rho$ in Table 10. The data

was analyzed, however, and some useful insight into the performance of the reflectance channels derived. From the analysis there is every expectation that the sensor will conform to the design goals (Table 9) once it is completed. The reflected return from a white wall situated 4.3 meters from the sensor was chosen for this evaluation since its characteristics most closely resembled a uniform reflectance standard when compared to all the other objects within the sensor FOV. The wall is seen in the foreground of the figures and is the dominant white region in the reflectance images. The standard deviation of the reflectance data of a section of the wall were within one count for each of the channels. This suggests that the NE$\Delta\rho$ of each channel is better than the resolvable 0.05 as expected. It was also observed that the fluctuations in the reflectance data from the green channel were considerably greater than the other two channels. This is expected since the doubled Nd:YAG beam had the greatest amplitude noise. Circuitry for compensating for the laser noise existed but was not operational during the laboratory data collection. It is believed that once the laser noise compensation circuitry is operational, the reflectance data will comply with the estimated performance.

TABLE 10.
SENSOR PERFORMANCE AS CALCULATED FROM LABORATORY SENSOR PARAMETERS

Wavelength	NEΔP	Power	Range for Specified NE$\Delta\rho$
0.53μm	0.002	0.9W	>75m
0.80μm	0.003	0.13W	50m
1.06μm	0.004	6.5W	>75m

(THIS PAGE INTENTIONALLY LEFT BLANK)

SECTION 6
CONCLUSIONS AND RECOMMENDATIONS

1. Fabrication of the main components of the MS-ALV sensor have been completed and preliminary laboratory testing indicates performance equal to, or greater than, that anticipated.

2. The size, weight and power consumption of the MS-ALV sensor are approximately as presented in the program design reviews; attempts were made to reduce the above parameters during fabrication but only limited success was achieved. Further investigations (see Appendix A) indicate the technology associated with diode-pumped lasers could now be utilized to significantly reduce all these parameters.

3. The MS-ALV sensor is a complex instrument and was given only limited testing utilizing regulated 3Φ laboratory power and controlled cooling for the lasers. The system should be subjected to extensive dynamic (ie, vehicle mounted) tests to fully characterize the instrument. Because of the size, weight and complexity of the system, it is considered to be relatively expensive to mount the sensor in the ALV and program economies may be realized by dynamic testing in a mobile laboratory already in existance at ERIM (see Section 4). On the completion of such tests, an informed decision could be made whether to redesign the system using alternative laser sources.

4. An active Multispectral Instrument has been fabricated for the ALV. However, only minimal effort has been expended on developing terrain classification

algorithms for use with the MS-ALV; this corollary effort needs to be implemented simultaneously with the initiation of field tests.

Pursuent to the above conclusions and recommendations ERIM submitted a detailed proposal to DARPA (ERIM #629112, June 1987) for a continuing effort in support of the ALV program. Primary and optional tasks in the proposed effort are outlined below:

PRIMARY PROGRAM TASKS

Task 1. Install and test the MS-ALV sensor system in a contractor instrumented vehicle. Tests shall include complete characterization and shakedown of the sensor. Results shall be furnished to the ALV System Integrator.

Task 2. Deploy the vehicle instrumented with the MS-ALV sensor to the ALV test site near Denver, Colorado and acquire representative MS-ALV sensor data at locations mutually agreeable to the sponsor and ERIM. A proposed test plan for on-site data acquisition shall be submitted to the sponsor and ALV system integrator for approval. Deployment on-site will be a maximum of ten days.

Task 3. Download all MS-ALV data acquired at the Denver test site to computer tape and reformat selected areas for dissemination of 4-6 copies to designated ALV system contractors. Reformatted data will be limited to 30 minutes of recorded data, e.g., ten 3-minute traverses over selected test sites. ERIM will also provide 6 copies of all TV video recorded in parallel with the MS-ALV.

Task 4. Provide engineering services related to the interface of MS-ALV system into the DARPA ALV. Support shall include up to two man-months of on-site effort at the ALV Systems Integrator facilities.

Task 5. Provide engineering support service and maintenance as required for the 3D sensor systems delivered on the DARPA ALV program. This is a level of effort task scoped to provide a total of 800 ±15% man-hours and necessary travel.

OPTIONAL TASKS

Task 0-1 Implement an algorithm development program for the MS-ALV sensor such that the algorithms could be integrated into the image processing system of the DARPA ALV. Algorithms will delineate combined MSS and 3D features necessary for route planning thereby permitting cross-country navigation. Algorithms shall be defined for and operational on ERIM equipment and delivered to the sponsor. Operation on sponsor equipment may require rewrite of software.

Task 0-2 Investigate alternative laser-diode pumped sources for the MS-ALV sensor. One or more diode-pumped source(s) will be selected for implementation on the MS-ALV sensor. The source(s) will be fabricated and laboratory tested to ensure power levels commensurate with MS-ALV requirements. The source design will be compatible with the MS-ALV sensor, however, optical alignment will be required and the installation may require sensor modification, possibly at ERIM's facilities. (Note: Due to rapid advancements in laser diode technology and uncertain component selection at this time, only budgetary

costs are included in the cost analysis of this proposal. A specific SOW and refined cost estimate will be submitted if/when this optional task is selected for implementation).

Task 0-3 Provide engineering services and technical support for the 3D and MS-ALV systems during FY89. Support would include maintenance of the 3D sensor systems delivered to OSU and CMU, as well as Martin Marietta. This will be a level of effort task providing 1600 ±15% man-hours and specified travel.

Task 0-4 Organize and conduct two workshops on 3D sensing technology to be held at contractors facilities during FY88. Agenda's for the workshop and invitees shall be approved by the sponsor.

Task 0-5 Organize and conduct two workshops related to multispectral sensors and associated processing technology. Workshops shall be held at contractors facilities with agendas for the workshop and invitees approved by the sponsor.

Task 0-6 Design and fabricate a refresh-window display for monitoring the image outputs of the MS-ALV sensor. System to be delivered to the ALV system integrator with appropriate technical documentation. Documentation will be to ERIM format and good commercial practice.

Task 0-7 Design and fabricate a digital recording unit (DRU) for recording the outputs of the MS-ALV sensor. System to be delivered to the ALV system integrator with appropriate technical documentation using ERIM format and good commercial practice.

Task 0-8 Prepare detailed documentation on the theory of operation of generic MS-ALV type sensors and their operating algorithms. (Note: Inclusion of discussion on algorithms requires implementation of optional task 0-1).

(THIS PAGE INTENTIONALLY LEFT BLANK)

LIST OF REFERENCES

1. "Strategic Computing", Defense Advanced Research Projects Agency Report, 28 October 1983.

2. Infrared and Optics Division, "Investigation of active/ passive line scan techniques", Technical Report AFAL-TR-75-162, Environmental Research Institute of Michigan, Ann Arbor, Michigan, January 1976.

3. Infrared and Optics Division, "Investigation of Iso-range Contour Sensor Techniques: a Target Height Cueing Sensor", Technical Report AFAL-TR-75-212, Environmental Research Institute of Michigan, Ann Arbor, Michigan, July 1976.

4. Larrowe, V.L., "Operating Principles of Laser-Ranging, Image-Producing (3D) Sensors, Report 628109-1-X, Environmental Research Institute of Michigan, Ann Arbor, Michigan, December 1986.

5. Zuk, David M., and Dell-Eva, Mark L., "Three-Dimensional Vision System for the Adaptive Suspension Vehicle", Report Number 170400-3-F, Environmental Research Institute of Michigan, Ann Arbor, Michigan, January 1983.

6. Zuk, D.M., Dell-Eva, M.L., and Van Atta, P., "3D Sensor for Adaptive Suspension Vehicle", Report Number 164700-4-F, Environmental Research Institute of Michigan, Ann Arbor, Michigan, November 1984.

7. Miller, C.D., "Image Sensor Data Base for the DARPA ALV Program", Report Number 193600-1-F, Environmental Research Institute of Michigan, Ann Arbor, Michigan, October 1986.

8. F. Thomson, R. Shuckman, K. Knorr, J. Ott, F. Sadlowski, "Studies of the Utility of Remotely Sensed Data for Making Mobility Estimates Using AMC Mobility Models", Report Number 14400300-2-F, NCSC Panama City, FL, November 1980.

9. J. Colwell, "Simulation of Reflection Properties of Selected Terrain Features Under a Variety of Viewing Conditions", ERIM Technical Report, March 1985.

REFERENCES CONT.

10. E.P. Crist and R.C. Cicone, "A Physically-Based Transfor-mation of Thematic Mapper Data--The TM Tasseled Cap", IEEE Trans. Geo. Rem. Sens. GE-22, 256 (1984)

11. R.J. Kauth and G.S. Thomas, "The Tasseled Cap--A Graphic Description of the Spectral-Temporal Development of Agricultural Crops as Seen by Landsat", in Proc. the Symposium on Machine Processing of Remotely Sensed Data, Purdue University, West Lafayette, Indiana, 4B-41 (1976).

12. A.R. Chraplyvy and T.J. Bridges "Infrared generation by means of multiple-order stimulated Raman scattering in CCl_4- and $CBrCl_3$- filled hollow silica fibers", Optics Letters 6, 632 (1981).

13. T.J. Bridges, A.R. Chraplyvy, J.G. Bergman, Jr., and R.M. Hart "Broadband infrared generation in liquid-bromine-core optical fibers", Optics Letters 7, 566 (1982).

14. C.D. Decker and P.J. Garner, "Efficient Raman/dye laser radiation source", Technical Report AFAL-TR-78-58 (1978); C.D. Decker, "High-efficiency stimulated raman scattering/ dye radiation source", Appl.Phys.Letter 33, 323 (1978).

APPENDIX A
DIODE PUMPED LASER RESEARCH

Recent advances in diode-pumped laser technology have created a new generation of efficient laser sources. Components are now readily available which can be used to construct laser systems with power levels compatible to many of ERIM's sensors. Technology exists today which did not exist last year when we were investigating sources for the MS-ALV. Now lasers can be built which would meet many of the wavelength and power requirements. High power laser diodes and new solid state crystals have been developed which offer a variety of wavelengths at power levels greater than 100mW. It is the purpose of this report to quantify some realistic levels and estimate costs of systems which can be constructed internally.

Diode-pumped lasers can be divided into two catagories according to the pump injection configuration. End-pumping occurs when the diode emission is injected into the ends of the laser crystal along the path of laser propagation. Transverse-pumping occurs when the pump is injected into the sides of the crystal perpendicular to the optical axis. End-pumping is the technique used in all commercially available systems. Discrete laser diodes must be used as the pump source. Power levels, therefore, are limited by discrete diode technology. Transverse-pumped systems, on the other hand, can use either a number of discrete diodes in a radial array or two-dimensional, high density diode arrays. Consequently, much higher power levels can be achieved with transverse-pumping.

---

* Excerpts from an ERIM Internal Memorandum regarding Status of Diode-Pumped Lasers

A schematic of an end-pumped system is given in Figure 1A. Up to four laser diodes can be used as a pump. Because laser diodes are inherently polarized, two of them can be coupled with polarization optics. In the four diode system, two pairs of polarization coupled diodes are injected into each end of the crystal. Dichroic surfaces are used to couple the diode energy into the cavity without coupling out the laser emission. If second harmonic generation (SHG) is desired a nonlinear crystal can be inserted in the cavity to take advantage of the high oscillating power levels existing there. All components for this system are available commercially.

Two transverse-pumped configurations are shown schematically in Figure 2A and 3A respectively. Figure 2A illustrates pumping with a radial array of discrete diodes. The diode energy is collimated and focused into the crystal rod from the sides. A large number of diodes can be arranged around the crystal. The maximum number is limited by how dense the arrangement can practically be made. As an example, researchers at Sanders Associates are testing a system with 10, 500mW diodes [1]. This system has the advantage that high power levels are achievable with components that are commercially available. Discrete diodes are the most expensive component of the system. Each time a diode is added the cost increases incrementally. There is a point where the cost will exceed the price of utilizing the high power, two-dimensional arrays which are available only through contract agreements at the present time. Figure 3A shows one of these arrays in an arrangement with a coupling lens into a solid state laser crystal slab. Such a configuration is utilized in the development efforts for slab lasers at McDonnell Douglas Astronautics Company [2].

Generating the most common Nd:YAG wavelength, 1.06um, with diode-pumping has been demonstrated many times.

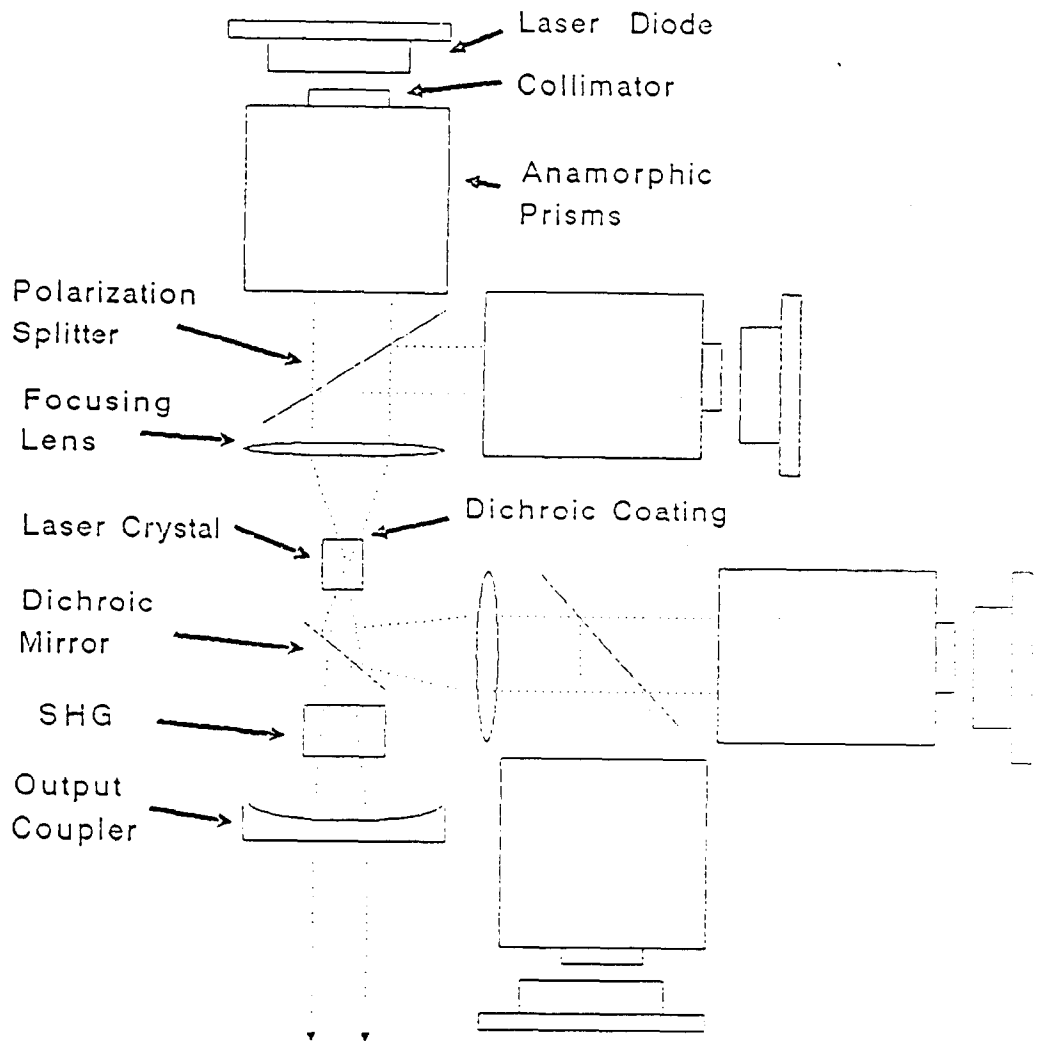

FIGURE 1A. END-PUMPED SOLID STATE LASER

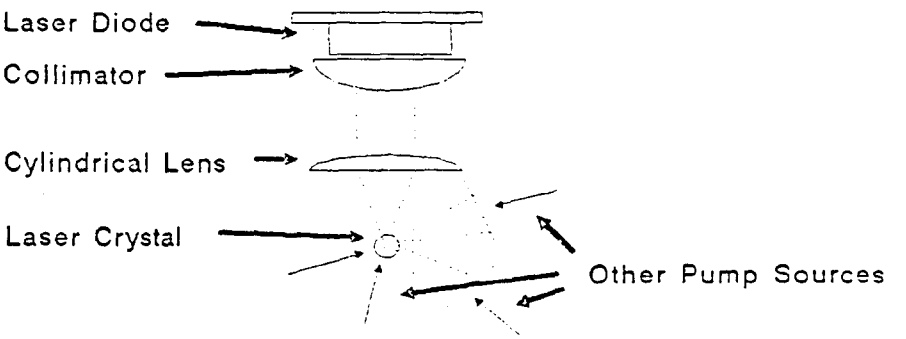

FIGURE 2A. TRANSVERSE PUMPING WITH DISCRETE DIODES

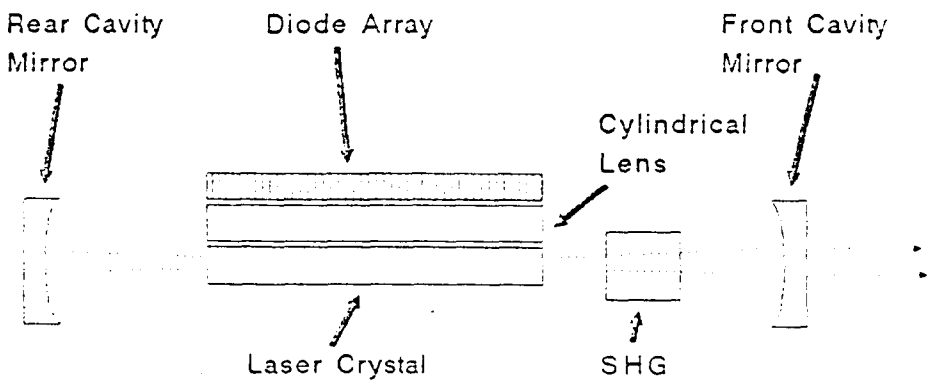

FIGURE 3A. TRANSVERSE PUMPING WITH A DIODE ARRAY

Several commercial systems are available today which operate at this wavelength. Spectra Physics, AB Lasers, and Lightwave Electronics have manufactured end-pumped systems that use either one or two diodes. Many incorporate second harmonic generation to produce 532nm. The Nd:YAG power levels available in the Spectra Physics lasers are presently rated at 70mW of 1.06um or 10mW of 532nm. these systems use two 200mW diodes which are polarization coupled.

The prospects for increasing the output power levels of diode pumped systems are tremendous. In flashlamp-pumped systems the power limitation is due to the thermal stresses induced in the crystal. The absorption band of the laser crystal is small in comparison to the flashlamp emission spectrum. Consequently, only a small percentage of the arclamp energy pumps the crystal. Most of it is converted to heat. In a diode-pumped system, pump efficiencies are high because the emission spectrum of the pump beam lies within the absorption band of the crystal. The heat generated in the crystal is small in comparison to an flashlamp-pumped system. The potential is therefore there to achieve greater output power levels with diode-pumped systems than with flashlamp-pumped systems. The limiting factor at present, is the cost to produce very high power diodes. Yet the rapid advances in semiconductor lasers continues to improve the power levels available. The diodes used in the systems today are rated at 200mW. Within the last two months, 1W laser diodes became available on the market. By next year, Spectra Diode Labs (SDL) predicts that 2W diodes will be available. In two years SDL speculates that 2W diodes will be available that have the same facet size as the present 200mW diode. This means that the systems sold today will be relatively easily upgraded an order of magnitude in power by replacing the laser diode. The same optics can be used. Increased power levels can

also be achieved with existing diodes by driving them beyond their rated limit. A large safety factor in the rating of SDL diodes allows them to be pushed to 2 to 3 times their rated power levels before catastrophic failure [3]. The lifetime of the diodes, however are reduced by approximately a factor of 25 when pushed to two times their rated power. For many applications this is not a concern since their lifetimes are on the order of 80 years to begin with.

In addition to the fundamental and second harmonic wavelengths generated in Nd:YAG, several other wavelengths in the visible, near-IR, and SWIR region are achievable with diode-pumped technology. Spectra Physics markets a Nd:YAG system which operated at 1.32um. Utilizing the same laser diodes the emission at 1.32um is 40% of the level attained at 1.06um. The production of 660nm radiation is possible through frequency doubling of 1.32um. Conversion efficiencies are approximately 15 to 20 percent [4]. in the MS-ALV sensor a goal of 200mW of 660nm radiation was established to meet the performance criterion. Achieving 200mW of 660nm, would require between 7W and 10W of pump power in Nd:YAG. Such levels would require 4, 1W diodes pushed to two times their rated level in an end-pumped system. The same levels can easily be generated with transverse-pumping without pushing the diodes. An alternative to Nd:YAG is the much more efficient Nd:YV04 under development at Aerospace Corporation [5,6]. Samples of the crystal may be available in six months. Their performance estimates indicate that between 2W and 2.75W of pump power will be required to generate 200mW of 660nm radiation. These levels are easily achieved in a 4-diode end-pumped system.

Several room temperature operated crystals have been developed with laser transitions in the near infrared. At

Stanford University a Tm:Ho:YAGH crystal has been demonstrated to produce 2.1um radiation at a 19% slope efficiency [7]. The requirement in the MS-ALV sensor was 100mW at this wavelength. this can be achieved with only 500mW of diode pump power. At Sanders Associates a Tm:YLF crystal has been demonstrated to produce 2.31um at a 15% slope efficiency [8]. They expect to improve this efficiency to 30% when the crystal is optimized. With 30% efficiency only 330mW of pump power would be required to produce 100mW output.

Other wavelengths are available at excellent efficiencies but the crystals require cooling with liquid nitrogen. Some examples are: HO:YLF @ 2.06um and Tm:YLF @ 1.88um [1].

An end-pumped system is the most conveniently fabricated because the parts are readily available and optical alignment is parallel to orthogonal axis. In Table 1, a parts list is given along with the actual cost for one, two, three, and four diode systems. Not included in the list are any of the mechanical mounts. The primary cost driver is the laser diode. The cost in parts for each system is approximately $10,000 per diode. The SHG option adds about $1000 to the cost of parts. Table 2A is a summary of the output levels achievable with various crystals and for each number of diodes. Laser diodes operating at their rated 500mW are used in the estimates. By operating the diodes at twice their rated power the output levels can be increased by approximately a factor of two. The power levels are characteristic of TEMoo mode operation. The summary indicates the tremendous potential of diode-pumped lasers. These lasers are extremely efficient, stable, and relatively simple to build.

For 3-D sensor applications a modulated laser is required to provide range-to-target information. Modulation of diode-pumped lasers can be achieved with the same techniques as flashlamp-pumped systems. The lasers can be modelocked and Q-switched. Recent advances in extra-cavity modulators has improved the modulation efficiencies at high frequencies. A new GaAs Bragg modulator has been developed with better than 90% diffraction efficiency and can modulate at rates up to 250MHZ. This is a tremendous breakthrough in acousto-optic modulators as previously such efficiencies could only be attained up to about 5MHZ. The device is manufactured by Brimrose. They claim it is good for wavelengths between 1um and 4um. There are, therefore, several good options for modulating the diode pumped systems.

Significant advances in solid state fiber lasers has occurred in the past year. The British have demonstrated diode pumped fiber lasers of several different wavelengths. The potential for such lasers is virtually untapped. One immediately apparent application is a wound cavity modelocked laser. By coiling the fiber the modelocked cavity length can be contained in a shorter physical space.

Table 1. Parts list for end pumped solid state lasers.

Part	(Qt.) Price 1 Diode	2 Diode	3 Diode	4 Diode
Laser Diode (SDL-2432-H1)	(1)7400	(2)14800	(3)22200	(4)29600
Collimator (06-GLC-002)	(1)168	(2)336	(3)504	(4)672
Anamorphic Prisms (06-GPA-002)	(1)265	(2)530	(3)795	(4)1060
Focusing Lens (06-GLC-004)	(1)139	(1)139	(2)278	(2)278
Solid State Crystal	(1)500	(1)500	(1)500	(1)500
Output Coupler	(1)250	(1)250	(1)250	(1)250
Polarization Splitter (03-PBS-062)	(0)0	(1)185	(1)185	(2)370
Dichroic Mirror	(0)0	(0)0	(1)300	(1)300
TEC Controller (LDC 201)	(1)600	(2)1200	(3)1800	(4)2400
Laser Diode Driver (LDD 100)	(1)995	(2)1990	(3)2985	(4)3980
Total without SHG	$10,317	$19,930	$29,797	$39,410
SHG Crystal (Cleveland Crystals)	(1)1026	(1)1026	(1)1026	(1)1026
Grand Total	$11,343	$20,956	$30,823	$40,436

Table 2. TEM_{oo} power levels attainable with end pumped solid state lasers using 500mW laser diodes.

Laser	um>um	n	1 Diode	2 Diode	3 Diode	4 Diode
Nd:YAG	.81>1.06	.33	.165	.330	.495	.660
(SHG)	1.06>.53	.15	.025	.050	.075	.100
	.81>1.32	.13	.065	.130	.195	.260
(SHG)	1.32>.66	.15	.010	.020	.030	.040
Nd:YV04	.81>1.06	.76	.380	.760	1.14	1.52
(SHG)	1.06>53	.15	.057	.114	.171	.228
	.81>1.32	.48	.240	.480	.720	.960
(SHG)	1.32>.66	.15	.036	.072	.108	.144
Tm:YLF	.78>2.3	.3	.150	.300	.450	.600
Tm:Ho:YAG	.78>2.1	.19	.095	.190	.285	.380

REFERENCES

1. Michael D. Thomas, Sanders Associates, Inc., Nashua (private communications.

2. Carolyn W. Krebs, McDonnel Douglas Astronautics Company, St. Louis (private communication).

3. Randy Klein, Spectra Diode Labs, San Jose (private communication).

4. Jim Doughman, Cleveland Crystals, Cleveland (private communication).

5. Randy A. Fields, Aerospace Corporation, Los Angeles (private communication).

6. R. A. Fields, M. Birnbaum, C. L. Fincher, "Highly efficient diode-pumped Nd:crystal lasers," in Conference on Lasers and Electro-Optics Technical Digest Series 1987, Vol. 14 (Optical Society of America, Washington, DC 1987), pp. 344-346.

7. T. Y. Fan, G. Huber, Robert L. Byer, "Continuous-wave diode-laser-pumped 2um Ho:YAG laser at room temperature," in Conference on Lasers and Electro-Optics Technical Digest Series 1987, Vol. 14 (Optical Society of America, Washington, DC 1987), p. 344.

8. M. D. Thomas, H. H. Zenzie, J. C. McCarthy, E. P. Chicklis, "Tm3+:YLF laser operation at 2.31um," in Conference on Lasers and Electro-Optics Technical Digest Series 1987, Vol. 14 (Optical Society of America, Washington, DC 1987), p. 240.

(THIS PAGE INTENTIONALLY LEFT BLANK)